



UNIVERSIDADE D
COIMBRA

João Daniel Machado Martins

**BI-OBJECTIVE ROBUST OPTIMIZATION FOR
THE POLLUTION-ROUTING PROBLEM
UNDER UNCERTAINTY IN TRAVEL TIME AND
DEMAND**

Dissertação no âmbito do Mestrado em Engenharia e Gestão Industrial orientada pelo Professor Doutor Telmo Miguel Pires Pinto e pelo Professor Doutor Carlos Alberto Henggeler De Carvalho Antunes e apresentada ao Departamento de Engenharia Mecânica da Faculdade de Ciências e Tecnologia da Universidade de Coimbra.

September of 2022



FCTUC FACULDADE DE CIÊNCIAS
E TECNOLOGIA
UNIVERSIDADE DE COIMBRA

DEPARTAMENTO DE
ENGENHARIA MECÂNICA

Otimização robusta para o problema bi- objetivo poluição-rotas com incerteza no tempo de viagem e na procura

Dissertação apresentada para a obtenção do grau de Mestre em Engenharia e
Gestão Industrial

**Bi-objective robust optimization for the pollution-routing
problem under uncertainty in travel time and demand**

Autor

João Daniel Machado Martins

Orientadores

Professor Doutor Telmo Miguel Pires Pinto

**Professor Doutor Carlos Alberto Henggeler De Carvalho
Antunes**

Júri

Presidente	Professor Doutor Samuel de Oliveira Moniz Professor da Universidade de Coimbra
Vogais	Professor Doutor Joana Maria Pina Cabral Matos Dias Professor Associada com Agregação da Universidade de Coimbra
Orientador	Professor Doutor Telmo Miguel Pires Pinto Professor Auxiliar da Universidade de Coimbra

Coimbra, September, 2022

“One repays a teacher badly if one always remains nothing but a pupil.”

Friedrich Nietzsche, in *Thus Spoke Zarathustra*, 1883.

To my family.

Page intentionally left blank.

Page intentionally left blank.

Resumo

Nos últimos anos, o problema de roteamento de veículos e o seu impacto ambiental tornou-se um ponto de interesse para as empresas logísticas e investigadores, que continuam a propor novas e mais completas formulações para este problema para melhor refletir o contexto real da operação logística. A incerteza inerente aos dados também levou ao aumento da investigação em modelos que consideram dados incertos, de modo a fornecer resultados aplicáveis na prática.

Nesta dissertação, estudamos o Problema de Rotas com Poluição, e propomos dois modelos que consideram a incerteza nos tempos de viagem e na procura, para os casos em que os custos ambientais e operacionais são uma preocupação, e estudamos os compromissos entre estes dois aspetos de avaliação. Verificamos que os atrasos na rota têm um impacto muito mais pronunciado nas emissões de veículos, nos custos operacionais, e nos tempos de resolução de problemas do que o aumento da procura. Mostramos também o impacto que os sistemas *start-stop* têm nos custos de operação, e como os reduzem sem esforço computacional extra. A interação entre o aumento da procura e os atrasos raramente é pronunciada, e, enquanto o aumento da procura tende apenas a piorar o desempenho ambiental, os atrasos conduzem a custos mais elevados e pior desempenho, devido ao aumento do salário do condutor, e ao aumento da velocidade dos veículos, o que leva a um aumento emissões.

Palavras-chave: Problema poluição-rotas, Rotas robustas, Otimização, Incerteza na procura, Incerteza no tempo de viagem, Bi-objetivo.

Abstract

In recent years, the Vehicle Routing Problem and its environmental impact have become a point of interest for logistic companies and researchers, that propose newer and more complete formulations to better reflect the real context of logistic operation. The inherent uncertainty in the data has also led to increasing research in models that work with uncertain data, as provide practical results.

In this dissertation, we study the Pollution Routing Problem, and propose two models that consider uncertainty in travel times and demand, for cases where environmental and operational costs are a concern and study the tradeoffs between the two. We find delays in route have a much more pronounced impact in vehicle emissions, operation costs, and in problem solving times than increase in demand. We also show the impact *start-stop* systems have on operation costs, and how they reduce them without requiring additional computational effort. The interaction between demand increase and delays is rarely pronounced, and, while demand increase tends to only worsen environmental performance, delays drive higher costs and worse performance, due to increase in driver pay, and increase in vehicle speeds, which leads to more emissions.

Keywords Pollution Routing Problem, Robust Routing, Optimization, Demand uncertainty, Travel time uncertainty, Bi-Objective.

List of Contents

FIGURE INDEX	xi
TABLE INDEX	xiii
ACRONYMS	xv
1. INTRODUCTION	1
1.1. Motivation and Objectives	2
1.2. Dissertation Structure	3
2. LITERATURE REVIEW	5
2.1. Green Logistics	5
2.2. Vehicle Routing Problem	5
2.2.1. Capacited Vehicle Routing Problem	6
2.2.2. Vehicle Routing Problem with Time Windows	6
2.3. Green Variants of the Vehicle Routing Problem	7
2.3.1. Green Vehicle Routing Problem	7
2.3.2. Pollution Routing Problem	8
2.4. Variants of the Pollution Routing Problem	9
2.4.1. Time-dependent Pollution Routing Problem	9
2.4.2. Fleet Size and Mix Pollution Routing Problem	11
2.4.3. Pollution Routing Problem with Simultaneous Pickup and Delivery	11
2.4.4. Bi-Objective Pollution Routing Problem	12
2.4.5. Bi-level Pollution Routing Problem	13
2.5. Uncertainty in Vehicle Routing Problem	14
2.5.1. Stochastic Routing	14
2.5.2. Robust Routing	16
2.5.3. Robust Routing in PRP	20
3. PROBLEM DESCRIPTION	25
3.1. Pollution Routing Problem	25
3.2. Robust Counterpart of the PRP formulation	29
3.2.1. Robust Pollution Routing Problem with Uncertain Demand	29
3.2.2. Robust Pollution Routing Problem with Uncertain Travel Time	30
3.2.3. Robust Pollution Routing Problem with Uncertain Travel Time and Demand	36
4. RESULTS	37
4.1. Data and Experimental Settings	37
4.2. Results of RPRP-TTD	38
4.2.1. RPRP-TTD with formulation I	38
4.2.2. RPRP-TTD with Formulation II	43
4.3. Results of Bi-Objective RPRP-TTD	45
4.3.1. Bi-Objective RPRP-TTD	46
4.3.2. Impact of increasing delay amount	47

- 5. CONCLUSION 51
 - 5.1. Main contributions..... 51
 - 5.2. Future Work..... 52
- REFERENCES..... 53

FIGURE INDEX

Figure 2.1. Fuel consumption at different speeds (Demir et al., 2012).....	9
Figure 2.2. Example of a PRPSPD solution (Tajik et al., 2014).....	12
Figure 2.3. Conceptual model for a Bi-level PRP (Qiu et al., 2020).....	13
Figure 2.4. Impact of increasing vehicle capacity in the OF (Tajik et al., 2014).....	23
Figure 3.1. Example of solution to a 4-node problem with Formulation II with the worst combination of s_{ij} highlighted.....	35
Figure 4.1. Reduction in operation costs resulting of shutting the engine down	40
Figure 4.2. Pareto fronts for 10-node instances under different levels of uncertainty	46
Figure 4.3. Pareto fronts for 20-node instances under different levels of uncertainty	47
Figure 4.4. Pareto fronts for a 10-node instance under maximum uncertainty with increasing delay amount.....	48
Figure 4.5. Pareto fronts for a 10-node instance under maximum uncertainty with increasing delay amount.....	49
Figure 4.6. Pareto fronts for a 20-node instance under maximum uncertainty with increasing delay amount.....	50

TABLE INDEX

Table 2.1. Impact of time period on vehicle speed (Moryadee et al., 2019).....	10
Table 2.2. Values taken by ψ for different robustness levels (Eshtehadi et al., 2017)	22
Table 3.1. Parameters used in instances	26
Table 4.1. Values of ψ and ϕ for different robustness levels	37
Table 4.2. OF values for the 10-node instances under some uncertainty	39
Table 4.3. OF values for the 10-node instances under maximum uncertainty	39
Table 4.4. Savings caused by shutting the engine down in 10-node instances	40
Table 4.5. Runtime values for 10-node instances under some uncertainty	41
Table 4.6. Runtime values for 10-node instances under maximum uncertainty	41
Table 4.7. OF values for 20-node instances under maximum uncertainty	42
Table 4.8. Savings caused by shutting the engine down 20-node instances	42
Table 4.9. CPU runtime values for 20-node instances under maximum uncertainty	43
Table 4.10. OF values for 10-node instances under some uncertainty	44
Table 4.11. Runtime values for 10-node instances under some uncertainty	44

ACRONYMS

VRP – Vehicle Routing Problem

CVRP – Capacitated Vehicle Routing Problem

VRPTW – Vehicle Routing Problem with Time Windows

GVRP – Green Vehicle Routing Problem

PRP – Pollution Routing Problem

ε – *CPRP* – Continuous Pollution Routing Problem

PRPSPD – Pollution Routing Problem with Simultaneous Pickup and Delivery

TWPDPRP – Time Window Pickup and Delivery Pollution Routing Problem

TDPRP – Time Dependent Pollution Routing Problem

FSMPRP – Fleet Size and Mix Pollution Routing Problem

RPRP – D – Robust Pollution Routing Problem with Uncertain Demand

RPRP – TT – Robust Pollution Routing Problem with Uncertain Time Travel

RPRP – TTD – Robust Pollution Routing Problem with Uncertain Time Travel

and Demand

SVRP – Stochastic Vehicle Routing Problem

CCP – Chance Constrained Programming

SPR – Stochastic Programming with Recourse

HWC – Hard Worst Case

SWC – Soft Worst Case

GHG – Greenhouse Gases

AFV – Alternative Fuel Vehicle

AFS – Alternative Fueling Station

DM – Decision Maker

OF – Objective function

RO – Robust Optimization

1. INTRODUCTION

The basic route planning problem, known as VRP, is becoming more well-known in today's distribution networks, due to rapid advancements in computational capabilities and solving methods, it is becoming feasible for companies to quickly design solutions for the collection or delivery of packages, which are carried out by a small fleet of vehicles, based on the geographic locations of customers, their respective demand, and time constraints.

The interest of companies in having off-the-shelf models and algorithms devoted to route planning problems is three-fold: not only can they optimize their transport system, reducing necessary manpower, improving customer satisfaction, and reducing costs, but also reduce the concerns caused by managing such complex networks of vehicles and customers. However, most models assume the information is perfect, that is, that the data provided to the model will materialize exactly, be it customer demands, travel speeds, travel times, fuel consumption (among others). The solutions provided by the models and algorithms reflect that assumption, but the solutions given are only guaranteed to work if the real world behaves exactly as expected, which is seldom case. That inherent uncertainty in the data has led to increasing research in approaches able to cope with uncertain data, as they better reflect real world conditions, and provide more usable results.

In this dissertation, we created models that consider uncertainty in travel times and demand, for cases where environmental, and operational costs are a concern. We study the impact that uncertain conditions have on solutions, and what trade-offs may exist between minimizing costs and minimizing emissions. We find delays in route have a higher impact in vehicle emissions and operation costs, as well as in problem solving times, than the increase in demand. We also show the impact start-stop systems have on operation costs, and how they reduce them. The interaction between demand increase and delays is rarely high, and, while demand increase tends to only worsen environmental performance, delays result in higher costs and worse performance, due to increase in driver's pay, and vehicle speeds, which leads to more emissions.

1.1. Motivation and Objectives

In recent years, the Vehicle Routing Problem (VRP) and the impact the transition to greener transportation systems has on the problem formulation has become a focus of researchers, leading to the introduction of more sophisticated formulations to the problem that allows for better reflecting the full context of the logistic operation (Peng et al., 2020). While the classic VRP is focused on reducing the economic cost of transporting a set of goods to a set of customers, more recent variations have begun to include green issues, such as the use of alternative fuel vehicles, pollution reduction, energy minimization, and other constraints, leading to more challenging optimization problems (Zhen et al., 2020).

During the last decades, the increase in emission of greenhouse gases (GHG) has become increasingly relevant. These GHG are mainly created by the burning of fossil fuels, which in turn are mainly consumed by the transportation sector, making this sector one of the main culprits of air pollution (Peng et al., 2020; Yu et al., 2020).

Meanwhile, consumer pressure and increasingly stiffer environmental regulations have led to many companies overhauling their logistic management (Peng et al., 2020), integrating environmental considerations into their logistic and vehicle route planning. In turn, this trend has led to the increase in the complexity of transportation optimization problems, caused by the potential dissonance between cost optimization and ecological optimization.

Therefore, this work establishes the main focus points:

1. Identify the main factors subject to uncertainty that affect vehicle routing problems.
2. Establish the conflicting objectives to evaluate solution in vehicle routing.
3. Formulate a model that is capable of handling uncertainty in a vehicle routing problem with environmental considerations.
4. Find the tradeoffs between handling uncertainty and optimal routing.
5. Find the impact of uncertainties on objective function tradeoffs.

1.2. Dissertation Structure

This dissertation contains 5 chapters. After this first introduction chapter, a literature review is presented, which consists of a study of Vehicle Routing Problem with focus on the Pollution Routing Problem and its variants, and a review of the main approaches to deal with uncertainty, with a focus on the robust programming methodology. In the third chapter, the problem formulations are presented, along with the explanations for the model components. The fourth chapter contains a series of computational results and their discussion. The fifth chapter presents the main conclusions, criticisms, and possible future developments of this work.

2. LITERATURE REVIEW

2.1. Green Logistics

(Poonthalir & Nadarajan, 2018) define Green Logistics as “routing vehicles with a concern towards environment”. Logistics are easily impacted by environmental factors, therefore routing vehicles should include concern towards environmental factors, particularly towards CO₂ emission reduction through the development of better operating plans. This has led carbon emission reduction to be intensively researched, and ingrained carbon emission as a day-to-day conversational theme (Peng et al., 2020). Research on green routing problems has then gained importance due to its environmental and societal impact.

Green Logistics has been widely researched in the literature, with particular attention paid to the environmental consequences of various distribution systems, waste management, energy conservation, and the use of unmanned aerial vehicles for delivery (Peng et al., 2020).

Under increasing petroleum prices, finding different sources of energy has been widely accepted as necessary. This makes Green Logistics an essential direction in the development of modern logistic solutions (Zhen et al., 2020).

The main types of problems of current research on Green Logistics are the Pollution Routing Problem, Energy Minimizing Vehicle Routing Problem, and Green Vehicle Routing Problem (Yu et al., 2020).

2.2. Vehicle Routing Problem

The Vehicle Routing Problem, as formulated by (Laporte, 1992), is the problem of, considering a depot, designing routes to deliver or collect a product to or from a set of customers distributed in a territory, subject to the following conditions.

1. Each customer must be visited only once and by one vehicle.
2. All vehicles start and end their route at the depot.

Initially described in (Dantzig & Ramser, 1959) the mathematical formulation of VRP now plays a central role in logistic planning.

2.2.1. Capacited Vehicle Routing Problem

An important extension of the VRP, the Capacitated Vehicle Routing Problem (CVRP) is formulated as a VRP with the following additional constraints ((Laporte, 1992).

1. Each customer has a non-negative demand that must be wholly fulfilled.
2. Each vehicle as a fixed maximum carrying capacity and may not leave the depot carrying more than said capacity.

2.2.2. Vehicle Routing Problem with Time Windows

(Cordeau et al., 1999) formulates the Vehicle Routing Problem with Time Windows (VRPTW) as an extension of the CVRP, in which the service to a customer has an associated time window in which the service must start and finish. Two types of time windows exist: soft time windows, which can be violated at a certain cost, and hard time windows, for which no violation is allowed.

For each i in a node set N there is an associated time window $[a_i, b_i]$, which represents the earliest and latest time at which service may start. If the vehicle arrives before the customer is ready to begin service, it waits. There is also a time window $[a_0, b_0]$, associated to the depot node, where the values represent the earliest departure possible from the depot, and the latest possible arrival to the depot.

Considering the travel time between node i and j to be t_{ij} and customer service time at node i to be s_i , the inclusion of time windows may reduce the number of solutions, and even lead to an impossible problem if (1) or (2) happen.

$$a_0 \leq \min (b_i - t_{0i}, i = 1, 2, \dots, |N|) \quad (1)$$

$$b_0 \geq \min(a_i + s_i + t_{i0}, i = 1, 2, \dots, |N|) \quad (2)$$

The problem is then formulated as a CVRP with additional constraints to account for service time constraints. The Objective Function (OF) is a minimization of total travel costs.

2.3. Green Variants of the Vehicle Routing Problem

2.3.1. Green Vehicle Routing Problem

Agencies consider numerous factors in the selection of a particular vehicle type, including fuel availability and geographic distribution of fueling stations in the service area, vehicle driving range, vehicle and fuel cost, fuel efficiency, and fleet maintenance costs. The lack of a national infrastructure for refueling alternative fuel vehicles (AFVs) presents a significant obstacle to alternative fuel technology adoption by companies and agencies seeking to transition from traditional petroleum-powered vehicle fleets to AFV fleets.

Moreover, existing alternative fueling stations (AFS) are distributed unevenly across the country and within specific regions. Additional operational challenges exist due to the reduced driving range of most AFVs, which, coupled with the lack of infrastructure, may increase the difficulties in overhauling conventional fleets for more modern, environmentally friendly ones (Erdoğan & Miller-Hooks, 2012).

As previously mentioned, transportation is responsible for a large part of GHG emissions. Furthermore, fuel consumption is a significant amount of the total cost of conventional transportation methods. The reduction of petroleum-based fuel consumption would therefore improve vehicle route efficiency. The Green Vehicle Routing Problem appears then with the goal of reducing fuel consumption and carbon emissions by using AFVs (Zhen et al., 2020).

However, the lack of large-scale infrastructure for AFV refueling creates operational problems unseen by conventional vehicle fleets, reducing the economic viability of overhauling conventional fleets for more modern, environmentally friendly ones (Erdogan, 2012).

Introduced by (Erdoğan & Miller-Hooks, 2012) the Green-Vehicle Routing Problem (GVRP) proposes the creation of routes of a fleet of homogenous vehicles, beginning and ending on a single depot, that pass through a subset of the existing vertices (which can be either customers or AFSs) with the main objective of reducing the total distance travelled.

2.3.2. Pollution Routing Problem

Before 2011, there was a gap in the application of energy-based models in vehicle routing, where GHG emissions, operational and economic objectives were all considered.

((Bektaş & Laporte, 2011) introduced the Pollution Routing Problem, which attempts to construct routes for a VRPTW model, with the objective to minimize the total cost composed of cost of emissions, operational costs and cost of drivers.

The PRP can be defined on a complete graph with a set of nodes and a set of arcs defined between each pair of nodes. Node 0 is the depot. There exists a homogeneous set of vehicles, each with a certain capacity. There is a customer set and every customer has a certain demand and a request to be served within a prespecified time interval. Each client requires a certain time to be served.

The PRP deals with constructing a set of routes for vehicles where:

1. Each customer has its demand fully fulfilled, is only visited by one vehicle, and has the service start at allowed times.
2. All vehicles depart from the depot and all vehicles must return to the depot at the end of their routes.
3. The depot has a minimum service time and maximum service time, which define the earliest start possible of the route and the maximum length of the route.
4. The speed at which a vehicle travels on arc is constrained by a lower bound and an upper bound.

The PRP formulation is non-linear due to the multiplication of speed and arc travel variables in the OF and the multiplication of node arrival time and arc travel variable in the calculation of driver time but can be linearized by discretizing the speed of a vehicle in each arc into R equally distant speed levels.

The fuel consumption formula proposed in (Bektaş & Laporte, 2011) fails to properly account for fuel consumption at lower speeds. (Demir et al., 2012) extend the PRP formulation, introducing a new term in the OF, that is only significant for lower speed levels, as shown in the dotted line in Figure 2.1, therefore better describing fuel consumption at speeds below 40 km/h.

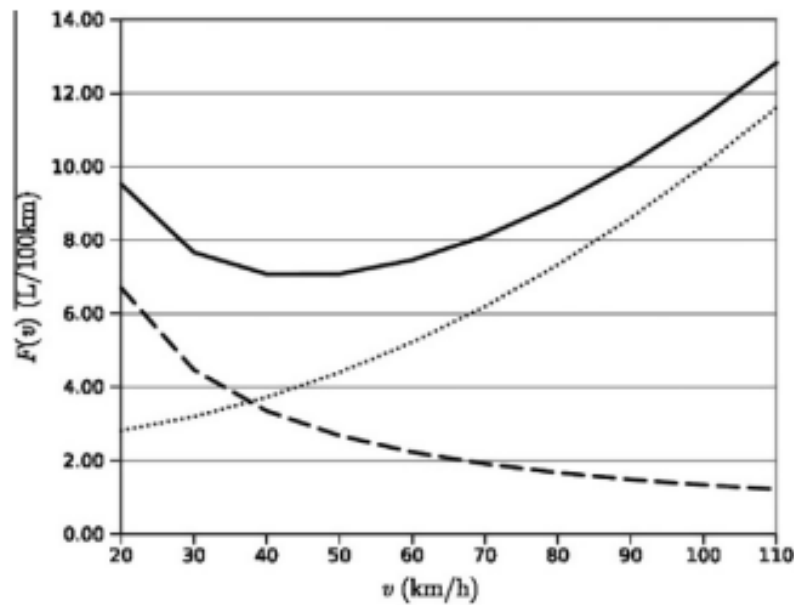


Figure 2.1. Fuel consumption at different speeds (Demir et al., 2012)

The discretization of speeds, although being a suitable tool to maintain linearity in the PRP formulation, leads to discretized travel times and fuel consumption rates, which increase the combinational complexity and may lead to sub-optimal solutions. (Xiao et al., 2020).

(Xiao et al., 2020) extended the PRP formulation to the continuous case, introducing the Continuous Pollution Routing Problem (ϵ -CPRP) by considering the travel speed as a continuous decision variable. All nonlinear components in the ϵ -CPRP are linearized by a unified parameter ϵ to control the approximation error, resulting in the model delivering truly optimized solutions. The authors find the parameter ϵ can be set as low as 0.01% without increasing the computational burden significantly and the gap between the solution found by the ϵ -CPRP model and the optimal one is within $3\epsilon\%$.

2.4. Variants of the Pollution Routing Problem

2.4.1. Time-dependent Pollution Routing Problem

Traffic congestion is a concern in many major cities throughout the world, especially during rush hours when traffic jams are common and delays likely. Increased

congestion also leads to increased exposure to some of the higher amounts of air pollution (Moryadee et al., 2019).

In the standard PRP formulation, the travel time of a vehicle is a function dependent on distance and speed, with the speed as an endogenous variable. In the Time-Dependent Pollution Routing Problem (TD-PRP), the speed also depends on the departure time of the vehicle because it is constrained during periods of traffic congestion.

Congestion can be considered in different ways. (Moryadee et al., 2019) define three time periods, seen in Table 2.1: a starting period where there is free flow, a congestion time period in the morning rush hour, and free-flow time period for the rest of the day.

Time Period	Average Vehicle Speed (km/h)
1:00 - 5:30 (Free-Flow)	60
5:30 - 10:00 (Congestion)	30
10:00 - 12:30 (Free-Flow)	60

Table 2.1. Impact of time period on vehicle speed (Moryadee et al., 2019)

Franceschetti et al (2013) assume there is an initial period of congestion, followed by free flow for the rest of the day. In the congestion period a vehicle drives at a congestion speed smaller than the speed limit, during the peak time, but is only limited by the speed limit in off-peak times. The authors assume congestion speed and congestions times are constant that are already known.

One characteristic of vehicle routing problems with time windows is the ability to arrive to a customer's location before the time window opens (with service only starting within the time window). However, these problems only allow for idle waiting before the service has begun, and do not consider waiting after a service has been completed as a congestion-reduction approach.

(Franceschetti et al., 2013) formulate the TDPRP as a PRP with special restrictions on vehicle speed. The authors employ the "idle waiting" technique to include congestion into the PRP framework, to appropriately account for the negative impacts of low speeds induced by congestion.

2.4.2. Fleet Size and Mix Pollution Routing Problem

Customer requests are addressed using heterogeneous vehicle fleets in most real-world distribution scenarios. The type of vehicle used has considerable influence on fuel usage, distance travelled, and CO₂ emissions, and is, therefore, an important variable to be studied.

Utilizing lower capacity trucks will likely increase overall distance travelled when compared to a heavy-duty vehicle fleet, but each heavy-duty vehicle comes with a larger engine, which results in higher fuel consumption and emissions per km. Replacing a large vehicle with many trucks of various types can reduce CO₂ emissions in some cases. Solving the Fleet Size and Mix Pollution Routing Problem (FSMPRP) is worthwhile for quantifying the benefits of using a flexible fleet in terms of fuel, emissions, and costs.

(Koç et al., 2014) introduced the FSMPRP, which is formulated as a PRP with the objective of minimizing the total cost, which includes vehicle, driver, fuel, and emissions costs. The maximum number of vehicles available for each type is imposed by constraints. They found that employing a heterogeneous fleet without speed optimization results in a higher decrease in overall cost than using a homogeneous fleet with speed optimization, also, considering appropriate fixed speed produces results that are just marginally worse than optimizing the speed on each arc.

2.4.3. Pollution Routing Problem with Simultaneous Pickup and Delivery

(Tajik et al., 2014) proposes the Pollution Routing Problem with Simultaneous Pickup and Delivery (PRPSPD), a variant of the PRP that includes two groups of nodes: the first contains customers whose loads should be picked up, and the second covers customers whose demands should be delivered. After servicing all pickup customers, their loads are carried by trucks that distribute the loads among delivery customers, an example of which can be seen in Figure 2.2. Hence, the amount of the product with which each vehicle is loaded up at the depot is the total demands of delivery nodes visited during their routes minus the total loads collected from pickup points in the routes that they are assigned to. If the total picked-up products are over or equal to the total delivery demands during the route the vehicle follows, it leaves the depot empty.

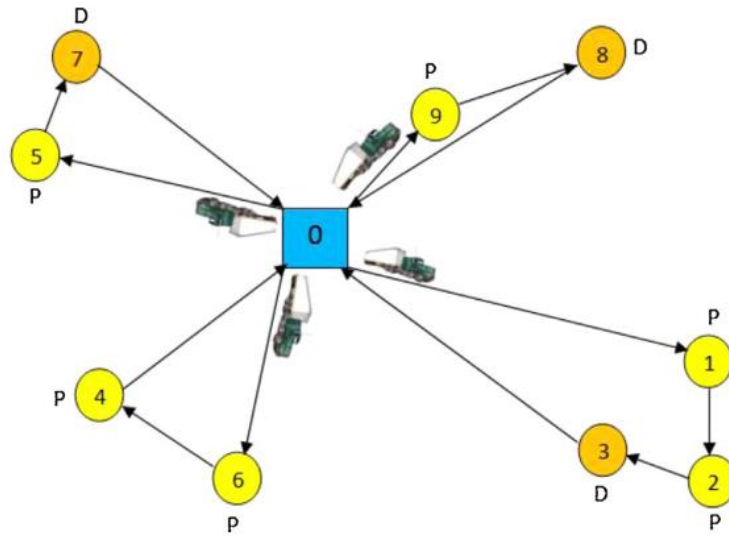


Figure 2.2. Example of a PRPSD solution (Tajik et al., 2014)

The PRPPD is formulated as a PRP with the added distinction of pickups from and delivery to customers considering soft time windows (with a penalty in the OF for earliness and tardiness).

2.4.4. Bi-Objective Pollution Routing Problem

Most real-world problems involve multiple objectives to evaluate the merit of solution, which are generally conflicting and incommensurate. In the VRP, there exists for each vehicle an optimal speed yielding a minimum fuel consumption, but that same speed is generally lower than the speed preferred by vehicle drivers in practice. Increasing vehicle speed leads to a reduction of total time spent on a route, which leads to the reduction of driver-associated costs, but this, in turn, increases fuel costs and emissions.

Since the two objectives of minimizing fuel and time are conflicting, using multi-objective optimization models and methods allows for an evaluation of the possible trade-offs. In the context of the PRP, (Demir et al., 2014) introduce the bi-objective PRP, consisting of a standard PRP problem where there are two conflicting objectives, namely the minimization of fuel consumption (using the fuel consumption formula presented in (Demir et al., 2012) and the total driving time.

The authors show that while the two objectives are conflicting, it is possible to achieve a strong reduction in fuel consumption without significantly increasing the total driving time, and vice-versa.

2.4.5. Bi-level Pollution Routing Problem

Bi-level optimization is most useful to model in situations where there is a leader-follower relation, meaning that the choices made by the leader restrict the follower's problem, the optimal solution of which has an impact on the leader's objective function.

(Nath et al., 2019) employed bilevel optimization in PRP where the customers are assigned to the fleet of vehicles by the depot, which operates as a leader. Its aim is to determine the number of vehicles needed and the assignment of vehicles to consumers. The vehicle will thereafter decide as the follower. Its goal is to plan a route that minimizes the overall distance travelled while considering the depot's choice. This approach, while bi-level in formulation, results in a pair of leader-follower that have similar priorities and are not affected by the choice of the other level, reducing the necessity of portraying this relation as a bi-level one.

Qiu et al (2020) also proposed a Bi-level PRP, seeking to minimize road freight transport carbon emissions by taking into account both the authority and the freight company, and their complex relationship, as seen in Figure 2.3.

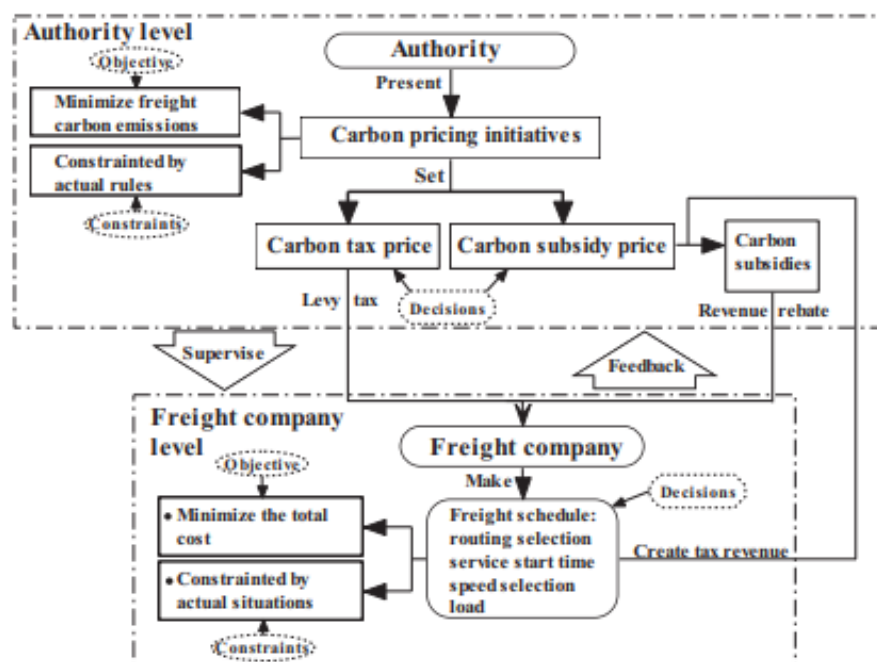


Figure 2.3. Conceptual model for a Bi-level PRP (Qiu et al., 2020)

In this model the authority sets prices for carbon emissions to minimize their cost, the freight company develops routes that minimize the total cost considering those emissions, which in turn leads to the authority changing the prices to again minimize carbon emissions. This back and forth continues until an equilibrium is reached between the upper and lower level objectives. Resolving disagreements between the authority and the freight business should be prioritized in order to jointly reduce road freight transport carbon emissions from the viewpoints of the authority and the freight company

2.5. Uncertainty in Vehicle Routing Problem

The consideration of uncertain parameters is a difficult aspect of the VRPs to solve. In order to address unknown events in demand, displacement time, and service time in a VRP, various approaches have been developed. The two main approaches - stochastic and robust techniques – are now distinguished.

The goal of the Stochastic Vehicle Routing Problem (SVRP) is to identify the objective function's near-best solution while accounting for all uncertain occurrences with defined probability distributions (Nasri, Hafidi, et al., 2020; Nasri, Metrane, et al., 2020).

However, in practice, one may not be aware of the travel and service timings ahead of time. Weather or traffic circumstances, for example, may cause travel durations between two vertexes to be uncertain. Furthermore, distribution technology, driver expertise, parking circumstances, and other factors may influence service times (Li et al., 2010).

A different strategy to deal with uncertain parameters is robust optimization, which does not rely on probability distributions for uncertain parameters, instead optimizing against the worst-case scenario that may be caused by the source of uncertainty, making the obtained solution as much as possible “immune” to it (Nasri, Hafidi, et al., 2020; Nasri, Metrane, et al., 2020).

2.5.1. Stochastic Routing

There is a striking difference between deterministic and stochastic VRP formulations: for all SVRP variants, the DM must decide the solution (at least partially) before the exact values of all parameters are completely known as these are independent continuous or discrete random variables with a probability distribution, such as uniform,

exponential, or normal (Li et al., 2010). The solution may fail when it is implemented with the realized data in opposition to the deterministic problem, where the DM has complete information when making the plans. There are two common ways of modelling stochastic problems: as a chance constrained program or as a stochastic program with recourse.

2.5.1.1. Chance Constrained Programming

Chance constrained programming (CCP) was proposed by (Charnes et al., 1959) as a method of stochastic programming. It provides a way of modelling stochastic decisions on the premise that the stochastic constraints will hold at least with probability α .

The problem is solved by ensuring that the probability of route failure is below a certain level and the cost of failures is typically ignored (Oyola et al., 2018). The objective is typically deterministic. The CCP model can be generically written as

$$\begin{aligned} & \text{Min } f(x) \\ & \text{Subject to} \\ & \text{Prob } (x \in X) \geq 1 - \alpha \end{aligned} \quad (3)$$

The DM provides the parameter value α giving the acceptable probability of failing to meet the constraints. The confidence level also influences the problem tightness, computational difficulty, and feasibility. A large enough confidence level may lead to unrealistic solutions (Oyola et al., 2018).

2.5.1.2. Stochastic Programming with Recourse

Although simple, the CCP model does not consider the possibility of route failure, nor does it take into account the correction costs in case of route failure (Li et al., 2010). In Stochastic Programming with Recourse (SPR), one allows route failures, but the DM must define a recourse policy, describing what actions to take to repair the solution after a failure (Oyola et al., 2018).

The recourse policy leads to different variants of an SVRP formulation. Three common recourse policies are:

1. When capacity is exceeded when servicing a customer, the vehicle interrupts its route and returns to the depot, resuming the route at the same customer.

2. Before route failure happens the vehicle preemptively travels to the depot. This method is averse to failure and attempts to prevent it from happening.
3. Each route is continuously optimized, and the vehicle path may change in route due to higher variations in demand than expected, route failure, or restocking.

2.5.2. Robust Routing

The most popular methods for coping with uncertainty are stochastic procedures, but they have two significant disadvantages: information accessibility and tractability. The first occurs when it is unknown what probability distribution describes the uncertain parameters, which frequently occurs when there is insufficient historical data. In addition, when there are many random variables, tractability may become a problem, making it prohibitively difficult to finish the optimization (Wang et al., 2021).

Robust optimization is an alternative paradigm that just assumes that uncertain parameters are expressed as variables that fall into a predetermined set, and searches for the best routing architecture that is immune to all possible parameter realizations within that set (Wang et al, 2021).

(Soyster, 1973) proposed a linear optimization model to construct a solution that is feasible for all data that belong to a convex set. The author considers the following nominal linear optimization problem.

Consider a row i of a nominal matrix A , with size $n * n$. Let J_i be the set of coefficients in row i that are subject to uncertainty. Each entry \bar{a}_{ij} , $j \in J_i$ takes values according to a symmetric distribution with a mean equal to the nominal value in the interval $[a_{ij} - \hat{a}_{ij}, a_{ij} + \hat{a}_{ij}]$. The authors formulate the linear model with auxiliary variable y_j as such.

$$\begin{aligned} & \text{Maximize} \quad \sum_{j=1}^n c_j x_j \\ & \text{subject to} \end{aligned}$$

$$\sum_{j=1}^n a_{ij}x_j + \sum_{j \in J_i} \hat{a}_{ij} y_j \leq b_i, \quad \forall i = 1, 2, \dots, n \quad (4)$$

$$-y_j \leq x_j \leq y_j, \quad \forall j = 1, 2, \dots, n \quad (5)$$

$$l_j \leq x_j \leq u_j, \quad \forall j = 1, 2, \dots, n \quad (6)$$

$$y_j \geq 0, \quad \forall j = 1, 2, \dots, n \quad (7)$$

At optimality, to allow x_j to take the greatest value possible y_j will be as low as possible, therefore $y_j = |x_j^*|$ which implies:

$$\sum_{j \in J_i} a_{ij}x_j^* + \sum_{j \in J_i} \hat{a}_{ij} |x_j^*| \leq b_i \quad \forall i = 1, 2, \dots, n \quad (8)$$

$\sum_{j \in J_i} \hat{a}_{ij} |x_j|$ gives the necessary protection to the i th constraint by maintaining a gap between $\sum_j a_{ij}x_j^*$ and b_i . The resulting model is capable of withstanding severe uncertainty; however, it produces considerably worse solutions, when compared to the deterministic problem, in order to ensure said robustness.

(Ben-Tal & Nemirovski, 2000) proposed a less conservative model by considering an uncertain linear problem, now with auxiliary variables u_{ij} and i_{ij} guaranteeing feasibility within an ellipsoidal uncertainty set.

$$\text{Maximize } \sum_{j=1}^n c_j x_j$$

subject to

$$\sum_{j=1}^n a_{ij}x_j + \sum_{j \in J_i} \hat{a}_{ij} u_{ij} + \Omega_i \sqrt{\sum_{j \in J_i} \hat{a}_{ij}^2 i_{ij}^2} \leq b_i, \quad \forall i = 1, 2, \dots, n \quad (9)$$

$$-u_{ij} \leq x_j - i_{ij} \leq u_{ij}, \quad \forall i, j \in J_i \quad (10)$$

$$l_j \leq x_j \leq u_j, \quad \forall j = 1, 2, \dots, n \quad (11)$$

$$u_{ij} \geq 0, \quad \forall i = 1, 2, \dots, n, \forall j = 1, 2, \dots, n \quad (12)$$

Where Ω_i is a positive number. The authors have shown that the probability that the i th constraint is violated is at most $e^{-\Omega^2/2}$. Models following ellipsoidal uncertainty are less conservative than the one proposed by (Soyster, 1973), as every feasible solution to the latter problem is a feasible solution to the former problem, but leads to nonlinear models, which are more demanding computationally (Bertsimas & Sim, 2004).

(Bertsimas & Sim, 2004) propose an approach for robust linear optimization that retains the linear formulation but offers control over the level of robustness of the solution.

Consider the i th constraint of the same nominal problem. For each i there is a parameter τ_i that governs the robustness of the solution and takes values in the interval $[0, |J_i|]$. The aim is to be protected against all cases when up to $\lfloor \tau_i \rfloor$ of these coefficients can change, and one coefficient a_{it} changes by $(\tau_i - \lfloor \tau_i \rfloor) * \hat{a}_{it}$, therefore, only a subset of the coefficients adversely affects the solution with the rest of the uncertain parameters taking their deterministic value.

The linear model is formulated as

$$\text{Maximize } \sum_{j=1}^n c_j x_j$$

Subject to

$$\sum_{j=1}^n a_{ij} x_j + z_i \tau_i + \sum_{j \in J_i} p_{ij} \leq b_i \quad \forall i = 1, 2, \dots, n \quad (13)$$

$$z_i + p_{ij} \geq \hat{a}_{ij} y_j \quad \forall j = 1, 2, \dots, n \quad (14)$$

$$-y_j \leq x_j \leq y_j \quad \forall j = 1, 2, \dots, n \quad (15)$$

$$l_j \leq x_j \leq u_j \quad \forall j = 1, 2, \dots, n \quad (16)$$

$$p_{ij} \geq 0 \quad \forall i, j \in J_i \quad (17)$$

$$y_j \geq 0 \quad \forall j = 1, 2, \dots, n \quad (18)$$

$$z_i \geq 0 \quad \forall i = 1, 2, \dots, n \quad (19)$$

The box, ellipsoidal and polyhedral sets can also be intersected to form new sets: “box+ellipsoidal”, “box+polyhedral” and “box+ellipsoidal+polyhedral” uncertainty sets, which are the intersection between ellipsoid and box, polyhedral and box, and ellipsoidal, polyhedral and box set, respectively.

(Li, Z., Floudas, 2012; Wang et al., 2021) study some of the most prevalent uncertainty sets used in the Robust Optimization (RO) literature considering consumer demand and vehicle travel time uncertainty and reduce the uncertainty sets studied by (Bertsimas & Sim, 2004).

The authors model the demand and travel time uncertainty as the following cardinality constrained sets.

$$Q_G := \{ q \in \mathbb{R}^n : q_i = q_i^0 + \hat{q}_i \varpi_i \forall i \in \{1, 2, \dots, n\}, \sum_{i=1}^n \varpi_i < \Gamma^q, \varpi_i \in [0, 1]^n \} \quad (20)$$

$$T_G := \{ t \in \mathbb{R}^n : t_{ij} = t_{ij}^0 + \hat{t}_{ij} \varsigma_{ij} \forall i, j \in A, \sum_{i=1}^n \varsigma_{ij} < \Gamma^t, \varsigma_{ij} \in [0, 1]^{n \times n} \} \quad (21)$$

Where N_0 is the set of customers, A is the set of arcs, q_i is the demand of customer i and t_{ij} is the travel time between node i and j . $q_i^0 \in \mathbb{R}_{>0}^n$, $\hat{q}_i \in \mathbb{R}_{>0}^n$, $\Gamma^q \in [0, |N_0|]$ and $t_{ij}^0 \in \mathbb{R}_{>0}^n$, $\hat{t}_{ij} \in \mathbb{R}_{>0}$, $\Gamma^t \in [0, |A|]$ are parameters that need to be specified by the modeler for the demand and travel time sets, respectively, and ϖ_i and ς_{ij} are variables indicating where demand or travel time worsening happen.

If the uncertainty sets Q_G and T_G are compact and convex, then they can be replaced by $\text{Ext}(Q_G)$ and $\text{Ext}(T_G)$ where $\text{Ext}(Q_G)$ or $\text{Ext}(T_G)$ denotes the set of extreme points of Q_G or T_G , respectively. The demand and travel time uncertainty sets can therefore be reduced to the sets of their extreme points.

Furthermore, if the uncertainty sets Q_G and T_G are compact and convex, then they can be replaced by $\overline{\text{Ext}}(Q_G)$ and $\overline{\text{Ext}}(T_G)$, where $\overline{\text{Ext}}(Q_G) \subseteq \text{Ext}(Q_G)$ and $\overline{\text{Ext}}(T_G) \subseteq \text{Ext}(T_G)$ denotes the set of non-dominated points of $\text{Ext}(Q_G)$ and $\text{Ext}(T_G)$, respectively.

Robust solutions following polyhedral uncertainty sets can provide good enough protection against uncertainty at a smaller cost premium over the deterministic situation (Rouky et al., 2018). Choosing the amount of uncertainty to consider is mostly left to the DM.

(Nasri, Hafidi, et al., 2020; Rouky et al., 2018) studied the VRPTW with uncertain travel and service times. The authors formulate two polyhedral uncertainty sets based on (Nasri, Metrane, et al., 2020), where the travel time interval $[t_{ij}, t_{ij} + \Delta_{ij} \varepsilon_{ij}]$ and the customer service time interval is $[P_i, P_i + \delta_i \omega_i]$, where t_{ij} and P_i denote the nominal values, and Δ_{ij} and δ_i are the maximum positive perturbations, and ε_{ij} and ω_i variables controlling the level of uncertainty. N is the set of nodes, W is the set of vehicles, and A is the set of arcs. They defined the sets U_t and U_p in a similar fashion as (20) and (21), respectively.

$$U_t = \{ \tilde{t} \in R^{|A|} / \tilde{t}_{ij} = t_{ij} + \Delta_{ij} \varepsilon_{ij} \sum_{(i,j) \in A} \varepsilon_{ij} \leq \Gamma, 0 \leq \varepsilon_{ij} \leq \Gamma, \forall (i, j) \in A \} \quad (1) \quad (22)$$

$$U_p = \{\tilde{P} \in R^{|M|} / \tilde{P}_i = P_i + \delta_i \omega_i \sum_{i \in N} \omega_i \leq \Lambda, 0 \leq \omega_i \leq \Lambda, \forall i \in N\} \quad (23)$$

Where Γ and Λ vary respectively between 0 and $|N| + |M|$, and 0 and $|N|$, and define the maximum number of travel times and customer service times that may be subject to uncertainty.

The model that guarantees the feasibility of a solution for all possible realizations of uncertain travel and service times is much harder to compute, as it may have to solve a model with as many as a very large number more scenarios.

(Munari et al., 2019) simplify the formulation of robust VRPTW models with travel time and demand uncertainty, reducing the complexity of formulating the constraints by adapting them to be Miller-Tucker-Zemlin (MTZ), introducing MTZ based constraints that guarantee feasibility for all realizations of uncertain travel time and demand without requiring the numerous constraints proposed by (Nasri, Hafidi, et al., 2020; Rouky et al., 2018).

2.5.3. Robust Routing in PRP

There is little literature relating to the implementation of robust PRP models.

(Eshtehadi et al., 2017) consider a special case of the PRP where the objective function solely depends on the total fuel consumption rather than the total cost of fuel consumed and driving time as in the PRP.

The authors formulate three models, each representing a different approach to robustness: the Hard Worst Case (HWC), a boxed uncertainty set that protects the solution for all possible realizations of q_i ; Soft Worst Case (SWC), which protects the solution for a certain number of realizations of q_i , and chance constrained robust model (which the authors classify as realistic approach), that protects the solution for $1-\alpha$ realizations of q_i .

The hard worst case robust optimization approach is modelled as a standard PRP problem with the following constraints added:

$$\sum_{j \in N} f'_{ij} - \sum_{j \in N} f'_{ji} = \bar{q}_i - \hat{q}_i \quad \forall i \in N_0 \quad (24)$$

$$\sum_{j \in N} f_{ij} - \sum_{j \in N} f_{ji} = \bar{q}_i + \hat{q}_i \quad \forall i \in N_0 \quad (25)$$

$$f_{ij}x_{ij} \leq (Q - \bar{q}_i - \hat{q}_i) x_{ij} \quad \forall i, j \in A \quad (26)$$

$$f_{ij}x_{ij} \geq (\bar{q}_j + \hat{q}_j) x_{ij} \quad \forall i, j \in A \quad (27)$$

$$f_{0j}x_{ij} \leq f'_{0j} \quad \forall i \in N_0 \quad (28)$$

$$\sum_{j \in N} f_{ij} - \sum_{j \in N} f_{ji} - \sum_{j \in N} f'_{ij} + \sum_{j \in N} f'_{ji} = 2\hat{q}_i \quad \forall i \in N \quad (29)$$

$$f'_{ij} \geq 0 \quad \forall i, j \in A \quad (30)$$

Where the continuous variable f'_{ij} is defined as the flow through the arc (i, j) in the worst-case scenario where each customer receives a lower bound of demand when vehicles are loaded with an upper bound of demand, f_{ij} is the flow through the arc (i, j) , \bar{q}_i is the nominal demand of customer i , \hat{q}_i is the variation in demand of customer i and x_{ij} is a binary variable that indicates whether arc between nodes i and j is travelled or not. Constraints (24)-(25) define the relation between f_{ij} and f'_{ij} , and together make the constraint (29) redundant. Constraints (26)-(27) define the flow through an arc when demands take their worst value, and constraints(28)-(30) guarantee f'_{ij} assumes only feasible values.

The soft worst-case robust optimization approach is modelled as PRP problem with the following constraints added.

$$\sum_{j \in N} f_{ij} - \sum_{j \in N} f_{ji} = \bar{q}_i + \Gamma_i \hat{q}_i \quad \forall i \in N_0 \quad (31)$$

$$f_{ij}x_{ij} \leq (Q - \bar{q}_i - \Gamma_i \hat{q}_i) x_{ij} \quad \forall i, j \in A \quad (32)$$

$$f_{ij}x_{ij} \geq (\bar{q}_j + \Gamma_i \hat{q}_j) x_{ij} \quad \forall i, j \in A \quad (33)$$

$$f_{0j}x_{ij} \leq f'_{0j} \quad \forall i \in N_0 \quad (34)$$

$$\sum_{j \in N} f_{ij} - \sum_{j \in N} f_{ji} - \sum_{j \in N} f'_{ij} + \sum_{j \in N} f'_{ji} = (1 + \Gamma_i) \hat{q}_i \quad \forall i \in N \quad (35)$$

$$\sum_{j \in N} \Gamma_i = \psi \quad (36)$$

$$\Gamma_i \in \{0,1\} \quad \forall i \in N_0 \quad (37)$$

Where binary variables Γ_i are defined in (37), and control the degree of conservation in each constraint i in which Γ_i is equal to 1 if customer i receives its upper bound value (otherwise it takes 0). The parameter ψ indicates how many uncertain variables

take their worst value and can be selected as any value in the interval $[0;|N|]$, and is given values representative of generic situations, as seen in Table 2.2. Constraints (31) and (35) are the SWC equivalent of (24) and (29). Constraints (32)-(33) are the SWC equivalent of (26)-(27), and define the flow through an arc when demands take either the worst value or the nominal value, indicated by variable Γ_i , which can only be 1 ψ times, guaranteed by constraint (36).

Instance Set	Values taken by ψ for different robustness levels			
	Zero	Low	Medium	High
UK10	0	2	5	7
UK15	0	3	7	11
UK20	0	5	10	15

Table 2.2. Values taken by ψ for different robustness levels (Eshtehadi et al., 2017)

The chance-constrained robust optimization PRP problem is modelled with the following constraints added.

$$\sum_{j \in N} f'_{ij} - \sum_{j \in N} f'_{ji} = \bar{q}_i - (1 - \alpha)\hat{q}_i \quad \forall i \in N_0 \quad (38)$$

$$\sum_{j \in N} f_{ij} - \sum_{j \in N} f_{ji} = \bar{q}_i + (1 - \alpha)\hat{q}_i \quad \forall i \in N_0 \quad (39)$$

$$\sum_{j \in N} f_{ij} - \sum_{j \in N} f_{ji} = \bar{q}_i + (1 - \alpha)\hat{q}_i \quad \forall i \in N_0 \quad (40)$$

$$f_{ij}x_{ij} \leq (Q - \bar{q}_i - (1 - \alpha)\hat{q}_i) x_{ij} \quad \forall i, j \in A \quad (41)$$

$$f_{ij}x_{ij} \geq (\bar{q}_j + (1 - \alpha)\hat{q}_j) x_{ij} \quad \forall i, j \in A \quad (42)$$

$$\sum_{j \in N} f_{ij} - \sum_{j \in N} f_{ji} - \sum_{j \in N} f'_{ij} + \sum_{j \in N} f'_{ji} = 2(1 - \alpha)\hat{q}_i \quad \forall i \in N \quad (43)$$

Where α is the chance of q_i taking its worst value, when demand follows a uniform distribution. Constraints (39)-(40) are the chance constrained equivalent of (24)-(25), with a similar redundancy appearing in (43), and constraints (41)-(42) are the chance constrained equivalent of (26)-(27).

The authors found that the robust solution leads to reliable routes, while only requiring a marginal increase in fuel consumption. Feasibility in all realizations of uncertain

values can be achieved with only a marginal increase in distance travelled and fuel consumed.

The authors also redefine the speed limits when studying travel time uncertainty, where low travel uncertainty is defined as $R = \{40; \dots; 75km/h\}$ whereas the high travel uncertainty is defined as $R = \{40; \dots; 55km/h\}$. However, this approach reduces the study of travel time uncertainty to the study of speed limit scenarios, which results in overconservative solutions (as in most cases not every road is constrained by the same speed limit) and does not account for delays that may happen when travelling.

(Tajik et al., 2014) study the Time Window Pickup and Delivery Pollution Routing Problem (TWPDPRP), extending the standard PRPSPD and guaranteeing the feasibility of the solution for all realizations of boxed uncertainty sets of service time, travel time, fuel cost and emissions cost.

After studying a specific instance, the authors found that increasing the capacity has no effect on the objective function until a certain size is reached, after which the increase in capacity allows for longer routes with one vehicle, which reduced the total cost of operation.

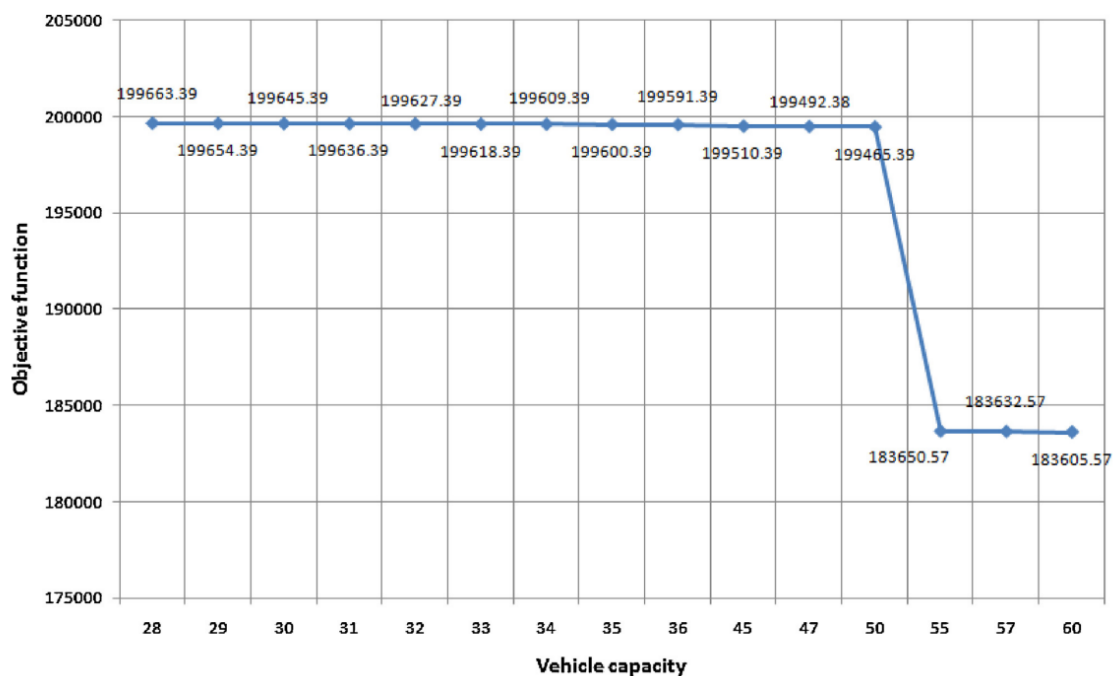


Figure 2.4. Impact of increasing vehicle capacity in the OF (Tajik et al., 2014)

Their findings corroborate the idea that one of the main cost drivers is the number of vehicles used. The authors also found, however, that certain cases exist where

smaller capacity constraints impose to much of a burden on fuel costs, leading to solutions with fewer vehicles being better. Figure 2.4 shows the optimal solution for different capacities, and although solutions using three or four vehicles exist at all capacity levels, the solution with four vehicles is more efficient until 55 tons capacity is reached.

3. PROBLEM DESCRIPTION

3.1. Pollution Routing Problem

The PRP is defined on a complete graph $G = (N; A)$ with $N = \{0, 1, 2, \dots, n\}$ as the set of nodes and A as the set of arcs defined between each pair of nodes. Node 0 is the depot. There exists a homogeneous set of vehicles W , each with capacity Q . The set $N_0 = \{1, 2, \dots, n\}$ is the customer set and every customer $i \in N_0$ has demand q_i and a request to be served within a prespecified time interval $[a_i, b_i]$. The time taken by a vehicle to serve customer i is denoted by t_i , and the distance from i to j is denoted by d_{ij} .

A binary variable x_{ij} is equal to 1 if a vehicle travels on arc $(i, j) \in A$. For a given arc $(i, j) \in A$, f_{ij} and v_{ij} respectively represent the amount of commodity flowing and the speed at which a vehicle travels on this arc. Variable y_j is the time at which service at node $j \in N_0$ starts, and s_j is the service time of the route with the last customer $j \in N_0$.

The fuel consumption formula used in this dissertation is presented in (Demir et al., 2012) and is calculated as the following:

$$F(v) = \lambda(kNV + w\gamma\alpha v + \gamma\alpha f v + \beta\gamma v^3) * \frac{d}{v} \quad (44)$$

where

$$\lambda = \frac{\xi}{\kappa\Psi} \quad (45)$$

$$\gamma = \frac{1}{1000 * \eta_{tf} * \eta} \quad (46)$$

$$\alpha = \tau + g \sin \theta + gC_r \cos \theta \quad (47)$$

$$\beta = 0.5 C_d \rho A \quad (48)$$

λ and γ are constants, α is an arc-specific constant and β is a vehicle-specific constant. f ; v ; τ ; θ ; d , w , denote the vehicle payload, vehicle speed, acceleration, road

gradient, distance, and curb weight of an empty vehicle, respectively. The definition of all parameters and their typical values are given in Table 3.1.

Table 3.1. Parameters used in instances

Notation	Description	Value used
ξ	Fuel-to-air mass ratio	1
k	Engine Friction Factor	0,2
N	Engine speed (rev/s)	33
V	Engine displacement(liters)	5
g	Gravitational constant (m/s^2)	9,81
C_d	Coefficient of aerodynamic drag	0,7
ρ	Air density (kg/m^3)	1,2041
A	Frontal surface area (m^2)	3,912
C_r	Coefficient of rolling resistance	0,01
n_{tr}	Vehicle drive train efficiency	0,4
η	Efficiency parameter for diesel engines	0,9
κ	Heating value of a typical diesel fuel (kJ/kg)	44
ψ	Conversion factor (g/s to L/s)	737
f_d	Driver wage (€/s)	0,0022
f_c	Fuel cost (€/L)	1,4
σ	Emission conversion factor ($kgCO_2eq/L$)	2,69212

There is a set of R equidistant non-decreasing speed levels $\bar{v}^r = \{1, 2, \dots, R\}$. A binary variable z_{ij}^r assumes 1 if a vehicle travels at speed level $r \in R$ on arc (i, j) , and 0 otherwise.

The standard PRP is then formulated:

$$\text{Minimize } \sum_{(i,j) \in A} f_c k N V \lambda d_{ij} \sum_{r=1}^R z_{ij}^r / \bar{v}^r \quad (49)$$

$$+ \sum_{(i,j) \in A} f_c w \gamma \lambda \alpha_{ij} d_{ij} x_{ij} \quad (50)$$

$$+ \sum_{(i,j) \in A} f_c \gamma \lambda \alpha_{ij} d_{ij} f_{ij} \quad (51)$$

$$+ \sum_{(i,j) \in A} f_c \beta \gamma \lambda \alpha_{ij} d_{ij} \sum_{r=1}^R z_{ij}^r (\bar{v}^r)^2 \quad (52)$$

$$+ \sum_{j \in N_0} f_d s_j \quad (53)$$

subject to

$$\sum_{j \in N} x_{j0} \geq 1 \quad (54)$$

$$\sum_{j \in N} x_{ij} = 1, \quad \forall i \in N_0 \quad (55)$$

$$\sum_{i \in N} x_{ij} = 1, \quad \forall j \in N_0 \quad (56)$$

$$q_j x_{ij} \leq f_{ij} \leq (Q - q_i) x_{ij}, \quad \forall (i, j) \in A \quad (57)$$

$$y_i - y_j + t_i + \sum_{r=1}^R d_{ij} z_{ij}^r - \bar{v}^r \leq M(1 - x_{ij}), \quad \forall i \in N, \forall j \in N_0, i \neq j \quad (58)$$

$$a_i \leq y_i \leq b_i, \quad \forall i \in N_0 \quad (59)$$

$$y_j - s_j + t_j + \sum_{r=1}^R d_{j0} z_{j0}^r / \bar{v}^r \leq M(1 - x_{j0}), \quad \forall j \in N_0 \quad (60)$$

$$\sum_{r=1}^R z_{ij}^r = x_{ij}, \quad \forall (i, j) \in A \quad (61)$$

$$f_{ij} \geq 0, \quad \forall (i, j) \in A \quad (62)$$

$$z_{ij}^r \in \{0, 1\}, \quad \forall (i, j) \in A, r = 1, 2, \dots, R \quad (63)$$

$$y_i - \sum_{j \in N} \sum_{r \in R} \max \left\{ 0, a_j - a_i + t_j + \frac{d_{ji}}{\bar{v}_r} \right\} z_{ji}^r \geq a_i, \quad \forall i \in N_0 \quad (64)$$

$$y_i + \sum_{j \in N} \sum_{r \in R} \max \left\{ 0, b_i - b_j + t_i + \frac{d_{ij}}{\bar{v}_r} \right\} z_{ij}^r \leq b_i, \quad \forall i \in N_0 \quad (65)$$

The objective function contains five components: (49) takes into account fuel consumption for speeds under 40 km/h, (50) and (51) measure the costs due to vehicle payload and curb weight, (52) measures the cost accrued by variations in speed. The last component (53) measures the total amount paid to the drivers. Constraint (54) means that at

least one vehicle departs from the depot. Constraints (55) and (56) guarantee that each customer is visited exactly once. The balance of flow is described through constraints (57) which model the flow as increasing by the amount of demand of each visited customer and having a hard limit in vehicle capacity. Constraints (58), (59) and (60) impose time window limits. Constraints (61) impose the choice of speed level in an arc, and that a speed level only exists if the arc is travelled by a vehicle. (62)-(63) define the variables f_{ij} and z_{ij}^r . Constraints (64)-(65) reduce solving times.

As stated in (Demir et al., 2014), increasing vehicle speed leads to the reduction of total time spent on a route, which leads to the reduction of driver-associated costs, but this, in turn, increases fuel costs and emissions. Two conflicting objective functions can then be defined, one pertaining to driver related costs, and one relating to emissions.

The bi-objective PRP can then be formulated as:

$$\text{Minimize } \sum_{(i,j) \in A} \sigma k N V \lambda d_{ij} \sum_{r=1}^R z_{ij}^r / \bar{v}^r \quad (66)$$

$$+ \sum_{(i,j) \in A} \sigma w \gamma \lambda \alpha_{ij} d_{ij} x_{ij} \quad (67)$$

$$+ \sum_{(i,j) \in A} \sigma \gamma \lambda \alpha_{ij} d_{ij} f_{ij} \quad (68)$$

$$+ \sum_{(i,j) \in A} \sigma \beta \gamma \lambda \alpha_{ij} d_{ij} \sum_{r=1}^R z_{ij}^r (\bar{v}^r)^2 \quad (69)$$

$$\text{Minimize } \sum_{j \in N_0} f_a s_j \quad (70)$$

Subject to (54)-(65)

3.2. Robust Counterpart of the PRP formulation

3.2.1. Robust Pollution Routing Problem with Uncertain Demand

We follow (Eshtehadi et al., 2017) to model for robust demand uncertainty. As described in Section 2.3.1, a parameter ψ is defined as an uncertainty budget, that states only a certain number of customers receive their upper bound value. Binary variables Γ_i reflect whether customer i receives the upper bound of its demand or not. Variable \hat{q}_i indicates the uncertain part of the demand of customer i , equal to 10% of q_i . According to the description of the SWC in 2.5.3, a new robust approach can be formulated as follows.

$$\text{Minimize } \sum_{(i,j) \in A} f_c k N V \lambda d_{ij} \sum_{r=1}^R z_{ij}^r / \bar{v}^r \quad (71)$$

$$+ \sum_{(i,j) \in A} f_c w \gamma \lambda \alpha_{ij} d_{ij} x_{ij} \quad (72)$$

$$+ \sum_{(i,j) \in A} f_c \gamma \lambda \alpha_{ij} d_{ij} f'_{ij} \quad (73)$$

$$+ \sum_{(i,j) \in A} f_c \beta \gamma \lambda \alpha_{ij} d_{ij} \sum_{r=1}^R z_{ij}^r (\bar{v}^r)^2 \quad (74)$$

$$+ \sum_{j \in N_0} f_a s_j \quad (75)$$

Subject to (54) – (56), (58) – (65), and

$$\sum_{j \in N} f_{ij} - \sum_{j \in N} f_{ji} = q_i + \Gamma_i \hat{q}_i, \quad \forall i \in N_0 \quad (76)$$

$$f_{ij} \leq (Q - q_i - \Gamma_i \hat{q}_i) x_{ij}, \quad \forall i, j \in A \quad (77)$$

$$f_{ij} \geq (q_j + \Gamma_i \hat{q}_j) x_{ij}, \quad \forall i, j \in A \quad (78)$$

$$f_{0j} \leq f'_{0j}, \quad \forall i \in N_0 \quad (79)$$

$$\sum_{j \in N} f_{ij} - \sum_{j \in N} f_{ji} - \sum_{j \in N} f'_{ij} + \sum_{j \in N} f'_{ji} = (1 + \Gamma_i) \hat{q}_i, \quad \forall i \in N \quad (80)$$

$$\sum_{i \in N_0} \Gamma_i = \psi \quad (81)$$

$$\Gamma_i \in \{0,1\}, \quad \forall i \in N_0 \quad (82)$$

Constraints (77)-(78) are the robust counterparts of constraint (57). (79) states that the worst-case value for flow must be equal or greater to the nominal flow. Constraints (76) and (80) define the relation between f_{ij} and f'_{ij} , (81) states that only ψ customers have increased demand and (82) defines the variables Γ_i .

This formulation is nonlinear due to (77) and (78), and is linearized by defining two new auxiliary variable sets, v and v' .

$$v_{ij} = \Gamma_i x_{ij} \quad (83)$$

$$v'_{ij} = \Gamma_j x_{ij} \quad (84)$$

and the following constraints

$$f_{ij} \leq (Q - q_i)x_{ij} - \hat{q}_i v_{ij}, \quad \forall (i, j) \in A \quad (85)$$

$$f_{ij} \geq q_j x_{ij} + \hat{q}_j v'_{ij}, \quad \forall (i, j) \in A \quad (86)$$

$$v_{ij} \leq x_{ij}, \quad \forall (i, j) \in A \quad (87)$$

$$v_{ij} \leq \Gamma_i, \quad \forall (i, j) \in A \quad (88)$$

$$\Gamma_i + x_{ij} \leq 1 + v_{ij}, \quad \forall (i, j) \in A \quad (89)$$

$$v'_{ij} \leq x_{ij}, \quad \forall (i, j) \in A \quad (90)$$

$$v'_{ij} \leq \Gamma_j, \quad \forall (i, j) \in A \quad (91)$$

$$\Gamma_j + x_{ij} \leq 1 + v'_{ij}, \quad \forall (i, j) \in A \quad (92)$$

$$v_{ij} \in \{0,1\}, \quad \forall (i, j) \in A \quad (93)$$

$$v'_{ij} \in \{0,1\}, \quad \forall (i, j) \in A \quad (94)$$

3.2.2. Robust Pollution Routing Problem with Uncertain Travel Time

3.2.2.1. Formulation I

In a similar fashion to Section 3.2.1 a new parameter ϕ can be defined to control the conservatism of the solution. Binary variables E_{ij} control the degree of conservation and assume the value of 1 if the arc suffers from a delay, and 0 otherwise. \hat{t} represents the amount of delay, in seconds.

Contrary to the demand uncertainty case, the travel time uncertainty was formulated as a constant increase in travel time instead of a percentual increase. This is because a delay in travel time is not necessarily larger the longer the travel is, contrarily to demand uncertainty, where it is more likely for a customer with an order of 5000 units to ask for 500 units more than it is for a smaller customer with an order of 500 units.

It is also necessary to quantify the impact a delay has on the objective function, which depends on what one considers a delay is: a reduction of speed in a subsection of the arc, a halting of the car with the engine running, or a complete stop with engine stopped. The complete stop without engine halting case was studied. The impact a full engine stop has on fuel consumption is obviously null, but the same does not apply when the engine is kept running.

When considering the halting of the car with the engine still running the impact the delay has on fuel emissions is independent of arc that suffers the delay.

Starting with the fuel consumption formula defined in (Demir et al., 2012)

$$FR(g/s) = \frac{\xi(KNV + P)}{k} \quad (95)$$

$$P = \frac{P_{tract}}{\eta_{tf}} + P_{acc} \quad (96)$$

$$P_{tract} = (M\tau + Mg \sin\theta + 0.5C_d\rho Av^2 + MGC_r \cos\theta) * \frac{v}{1000} \quad (97)$$

When the car suffers the delay it stops, therefore the speed when suffering the delay is 0.

$$v = 0 \Rightarrow P_{tract} = 0 \Rightarrow P = 0 \Rightarrow FR = \frac{\xi KNV}{k} \quad (98)$$

$$\text{Cost associated to a delay} = f_c * \frac{\xi KNV}{k} * \frac{1}{\psi} * E_{ij} * \hat{t} \quad (99)$$

$$\text{Cost associated with all delays} = \sum_{(i,j) \in A} f_c * KNV\lambda * E_{ij} * \hat{t} \quad (100)$$

In the cost associated with all delays only E_{ij} is a variable. Since

$$\sum_{(i,j) \in A} E_{ij} = \phi \quad (101)$$

The equation can be reduced to

$$\text{Cost associated with all delays} = f_c * KNV\lambda * \hat{t} * \psi \quad (102)$$

The definition of the delay value also deserves attention. In the real world, a delay may be anything from a few minutes to several hours. While the impact of increasing delay amounts is also studied, for simplicity's sake, the delay was set as 20% of the average travel time in all arcs in a certain instance, calculated as the average of distances/average speed, then rounded to 1000 seconds.

The SWC delay formulation is as follows:

$$\text{Minimize } \sum_{(i,j) \in A} f_c k N V \lambda (d_{ij} \sum_{r=1}^R z_{ij}^r / \bar{v}^r + \hat{t} E_{ij}) \quad (103)$$

$$+ \sum_{(i,j) \in A} f_c w \gamma \lambda \alpha_{ij} d_{ij} x_{ij} \quad (104)$$

$$+ \sum_{(i,j) \in A} f_c \gamma \lambda \alpha_{ij} d_{ij} f_{ij} \quad (105)$$

$$+ \sum_{(i,j) \in A} f_c \beta \gamma \lambda \alpha_{ij} d_{ij} \sum_{r=1}^R z_{ij}^r (\bar{v}^r)^2 \quad (106)$$

$$+ \sum_{j \in N_0} f_d s_j \quad (107)$$

Subject to (54),(56) - (57),(59),(61) - (63)

And

$$y_i + t_i + \sum_{r=1}^R \left(d_{ij} * \frac{z_{ijr}}{v_r} \right) + E_{ij} * \hat{t} \leq M * (1 - x_{ij}) + y_j, \quad \forall (i,j) \in A \quad (108)$$

$$y_j + t_j + \sum_{r=1}^R \left(d_{j0} * \frac{z_{j0r}}{v_r} \right) + E_{j0} * \hat{t} \leq M * (1 - x_{j0}) + s_j, \quad \forall (i,j) \in A \quad (109)$$

$$E_{ij} \leq x_{ij}, \quad \forall (i,j) \in A \quad (110)$$

$$\sum_{i,j \in A} E_{ij} = \phi \quad (111)$$

$$E_{ij} \in \{0,1\}, \quad \forall (i,j) \in A \quad (112)$$

$$\phi \in \{0,1, \dots, |N| + |W|\} \quad (113)$$

Constraints (108) - (109) are the robust counterparts of (58) and (60). Constraint (110) guarantees that a delay only occurs on travelled arcs, and constraint (111) defines only ϕ arcs suffer delays. Constraints (112)-(113) define E_{ij} and ϕ .

3.2.2.1. Formulation II

While simpler to study and implement, the previous formulation for the time travel delay has the variables that represent the choice of where the delay happens as endogenous, meaning the model chooses where the delays happen, therefore, when only some arcs suffer delay, the models cannot guarantee the feasibility of a solution for all possible combinations of delays (equivalent to ensuring feasibility inside a polyhedral uncertainty set). Another formulation, derived from (Munari et al., 2019), which can guarantee feasibility inside a polyhedral uncertainty set, is proposed.

Variables y_j and s_j are replaced by y_{jn} and s_{jn} , respectively, where y_{jn} is the time service starts at j when n arcs have suffered delays, and s_{jn} is the service time of the route with the last customer being j when n arcs have suffered delays.

The model is defined as follows.

$$\text{Minimize } \sum_{(i,j) \in A} f_c w \gamma \lambda \alpha_{ij} d_{ij} x_{ij} \quad (114)$$

$$+ \sum_{(i,j) \in A} f_c \gamma \lambda \alpha_{ij} d_{ij} f_{ij} \quad (115)$$

$$+ \sum_{(i,j) \in A} f_c \beta \gamma \lambda \alpha_{ij} d_{ij} \sum_{r=1}^R z_{ij}^r (\bar{v}^r)^2 \quad (116)$$

$$+ \sum_{(i,j) \in A} f_c k N V \lambda (d_{ij} \sum_{r=1}^R z_{ij}^r / \bar{v}^r) \quad (117)$$

$$+ f_c k N V \lambda * \hat{t} * \phi \quad (118)$$

$$+ f_d H \quad (119)$$

Subject to (54)-(57),(59),(61),(62),(63) and

$$y_{in} + t_i + \sum_{r=1}^R \left(d_{ij} * \frac{z_{ijr}}{v_r} \right) \leq M * (1 - x_{ij}) + y_{jn}, \quad \forall (i,j) \in A, n \in \{0,1, \dots, \phi\} \quad (120)$$

$$y_{in-1} + t_i + \sum_{r=1}^R \left(d_{ij} * \frac{z_{ijr}}{v_r} \right) + \hat{t} \leq M * (1 - x_{ij}) + y_{jn}, \quad \forall (i,j) \in A, n \in \{0,1, \dots, \phi\} \quad (121)$$

$$y_{jn} + t_j + \sum_{r=1}^R \left(d_{j0} * \frac{z_{j0r}}{v_r} \right) \leq M * (1 - x_{j0}) + s_{jn}, \quad \forall (i, j) \in A, n \in \{0, 1, \dots, \phi\} \quad (122)$$

$$y_{jn-1} + t_j + \sum_{r=1}^R \left(d_{j0} * \frac{z_{j0r}}{v_r} \right) + \hat{t} \leq M * (1 - x_{j0}) + s_{jn}, \quad \forall (i, j) \in A, n \in \{0, 1, \dots, \phi\} \quad (123)$$

$$a_i < y_{in} < b_i, \quad \forall i \in N_0, n \in \{0, 1, \dots, \phi\} \quad (124)$$

$$a_0 < s_{in} < b_0, \quad \forall i \in N_0, n \in \{0, 1, \dots, \phi\} \quad (125)$$

$$H \geq \sum_j s_{jn_j}, \quad \forall n_j \in \{0, 1, \dots, \phi\} \mid j \in N_0 \wedge \sum_j n_j = \phi \quad (126)$$

Constraints (120) and (121) recursively define the arrival time at a customer as the highest of two cases: either all n delays have happened, and the path between the last customer and i suffers no delay, or only $n - 1$ delays had happened, and the path between the last customer and customer i suffers a delay. Constraints (122) and (123) define s_{jn} in a similar way, and allow for the model not having an extra node for the depot, as created in (Munari et al., 2019).

Constraints (124) and (125) guarantee feasibility for all possible realizations of the delay.

This model better adheres to the previously mentioned concept budget uncertainty but obtaining the service time for (119) is significantly more challenging, as we now have a collection of service times to choose from. Since robustness refers to minimizing the worst case, the model must select the set of service times with the largest sum, where the sum of all second indexes equals ϕ , this was implemented in (126).

A representation of the problem created is shown in Figure 3.1 which features a feasible solution with three routes to a hypothetical four customer problem where two arcs suffer a delay.

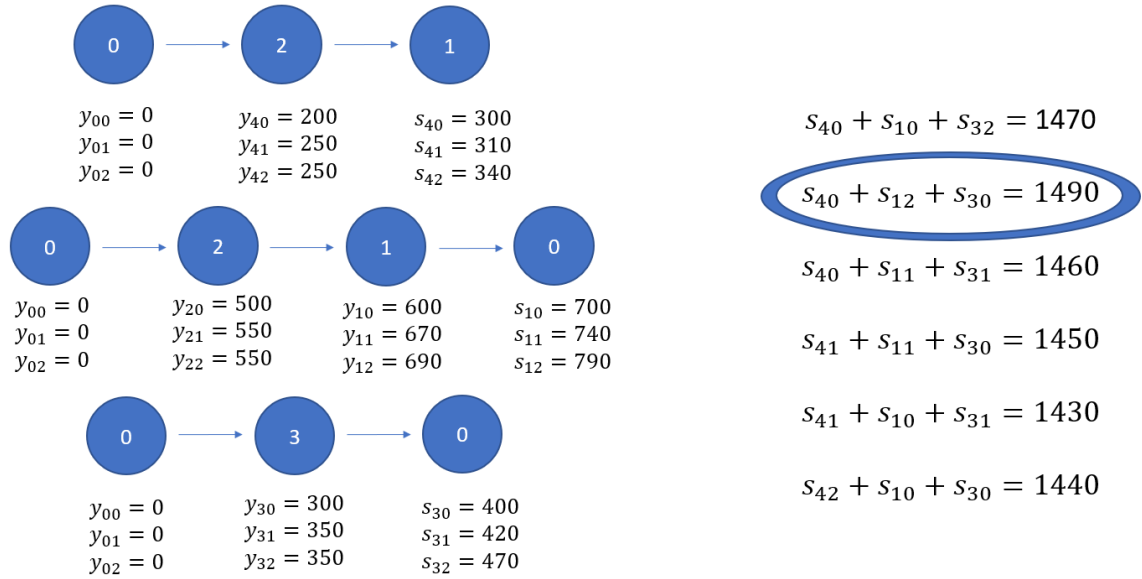


Figure 3.1. Example of solution to a 4-node problem with Formulation II with the worst combination of s_{ij} highlighted

To obtain the value of (119) one must search for all possible combinations of one s_{1n}, s_{3n} and s_{4n} where the sum of all n indexes is two. This can be generalized to obtain the number of constraints introduced by (126), since it involves choosing one value of $\phi + 1$ possibilities, $|N_0|$ times, which means it will introduce no more than $(\phi + 1)^{|N_0|}$ constraints, an amount that quickly gets prohibitively complicated to handle.

There are some techniques that can help reduce the amount of possibilities: every combination where there is at least one s_{in} where n is greater than 0 and the node i is not the last customer in a route can be discarded, as one can easily obtain a total sum equal or greater with the combination where all n delays present in s_{in} are allocated to a different route service time where the corresponding node is the last in a route. While theoretically helpful, we were not able to define the corresponding formulation and computational implementation. Also, the existence of multiple service times and the choice that must be made make the use of (64) and (65), impossible in this model, which results in even worse performance.

3.2.3. Robust Pollution Routing Problem with Uncertain Travel Time and Demand

The formulations in Section 3.2.1 and Section 3.2.2.1 can be joined in order to create a model robust to both demand and travel time uncertainty.

$$\text{Minimize } \sum_{(i,j) \in A} f_c w \gamma \lambda \alpha_{ij} d_{ij} x_{ij} \quad (127)$$

$$+ \sum_{(i,j) \in A} f_c \beta \gamma \lambda \alpha_{ij} d_{ij} \sum_{r=1}^R z_{ij}^r (\bar{v}^r)^2 \quad (128)$$

$$+ \sum_{(i,j) \in A} f_c \gamma \lambda \alpha_{ij} d_{ij} f'_{ij} \quad (129)$$

$$+ \sum_{(i,j) \in A} f_c k N V \lambda (d_{ij} \sum_{r=1}^R z_{ij}^r / \bar{v}^r + \hat{t} E_{ij}) \quad (130)$$

$$+ \sum_{j \in N_0} f_d S_j \quad (131)$$

Subject to (54)-(56),(59),(61),(63)-(65),(76)- (82),(85)-(94),(108)-(113)

And its bi-objective counterpart.

$$\text{Minimize } \sum_{(i,j) \in A} \sigma w \gamma \lambda \alpha_{ij} d_{ij} x_{ij} \quad (132)$$

$$+ \sum_{(i,j) \in A} \sigma \beta \gamma \lambda \alpha_{ij} d_{ij} \sum_{r=1}^R z_{ij}^r (\bar{v}^r)^2 \quad (133)$$

$$+ \sum_{(i,j) \in A} \sigma \gamma \lambda \alpha_{ij} d_{ij} f'_{ij} \quad (134)$$

$$+ \sum_{(i,j) \in A} \sigma k N V \lambda (d_{ij} \sum_{r=1}^R z_{ij}^r / \bar{v}^r + \hat{t} \Gamma_{ij}) \quad (135)$$

$$\text{Minimize } \sum_{j \in N_0} f_d S_j \quad (136)$$

Subject to (54)-(56),(59),(61),(63)-(65),(76)- (82),(85)-(94),(108)-(113)

4. RESULTS

4.1. Data and Experimental Settings

In order to validate the proposed mathematical models, we resort on the library created by (Demir et al., 2012), whose instances represent randomly selected cities from the UK and use real geographical distances. All instances are available for download from <http://www.apollo.management.soton.ac.uk/prplib.htm>. Implementations of all formulations were done in Python, using the Python CPLEX API to interact with CPLEX. Preliminary analysis was conducted on a PC with an i7-4720hq and 8GB of RAM. Experiments were conducted on a server with an Intel Xeon Gold 6138@3.7GHz processor and 320GB of RAM.

All parameters were used as previously defined in Table 3.1. There was a three-hour time limit on each run. Unless indicated otherwise, a problem ran until optimality was achieved. Instances that reached the time limit have the corresponding gap to the best possible solution indicated. Studying all possible cases of uncertainty would be excessive, and generate too much information, making it difficult to draw conclusions, therefore we choose to use values that represent some plausible level uncertainty and maximum uncertainty, which are show in Table 4.1.

Table 4.1. Values of ψ and ϕ for different robustness levels

Instance Set	Value of ψ for different robustness levels			Value of ϕ for different robustness levels		
	Det	Avg	Max	Det	Avg	Max
UK10	0	5	10	0	6	12
UK20	0	10	20	0	12	23

For demand uncertainty we considered maximum uncertainty when all customers take their worst values, and some level of uncertainty as half (rounded up) of the customers take their worst values. Travel time uncertainty is more challenging, as the total amount of arcs run by vehicles is equal $|N_0| + |W|$, however, the number of vehicles is an endogenous variable, which means the maximum number of arcs is only known after the instance is run. The maximum number of arcs cannot be known, but a minimum to this value

can, since each car has a certain capacity and all customer demand has to be met. The minimum number of vehicles used can be derived by dividing the sum of all demands and the capacity of a single vehicle and rounding up the result. This means we can obtain a minimum number of arcs travelled, which is used when the maximum number of arcs suffers the delay, and half of that is used when some arcs suffer delay.

4.2. Results of RPRP-TTD

4.2.1. RPRP-TTD with formulation I

The following tables show the solutions to 10 and 20 node instances of the PRP. Ten instances were run for each node count. All problems with 10 nodes ran to optimality, while no optimal solution could be reached with any of the 20-node problems. Table 4.2 and Table 4.3 show the OF values for the 10-node instances under some and maximum uncertainty, and Table 4.5 and Table 4.6 show the CPU runtimes for the corresponding instances. Table 4.7 and Table 4.8 show the OF values and CPU runtimes for the 20-node instances under maximum uncertainty.

In the following tables, “*OF*” represents the value obtained for the objective function, and “*%OF*” represents the percentual difference between the objective function value from a certain instance to the objective function value of corresponding deterministic problem. Similarly, “*Time*” represents the time spent in seconds by the CPU to obtain the optimal solution, and “*%Time*” is the percentual difference between time from a certain instance and the time in the corresponding deterministic problem. Each couple of numbers represents the value of uncertain parameters used in the columns directly below – the left number corresponding to the amount of demand uncertainty ψ , and the right number to the amount of travel time uncertainty ϕ .

Table 4.2. OF values for the 10-node instances under some uncertainty

Uncertainty Values	Deterministic		RPRP-D		RPRP-TT		RPRP-DTT	
	0	0	5	0	0	6	5	6
Problem	OF		OF	%OF	OF	%OF	OF	%OF
10_1	171		172	0,36	192	12,40	193	12,76
10_2	205		206	0,26	226	10,23	227	10,49
10_3	200		201	0,20	221	10,09	221	10,29
10_4	190		191	0,26	211	10,75	211	10,98
10_5	176		176	0,23	197	12,17	197	12,39
10_6	215		215	0,16	234	9,11	234	9,28
10_7	190		191	0,22	212	11,43	212	11,64
10_8	223		223	0,33	244	9,77	245	10,10
10_9	175		175	0,19	196	12,45	197	12,64
10_10	190		191	0,27	212	11,44	212	11,71
Average	193		194	0,25	215	10,98	215	11,23
Std.Deviation	16,39		16,43		16,15		16,19	

The 10-node instances under some uncertainty show on average a 0.25% worsening of the objective function value when only demand uncertainty is concerned, while delays in travel time result in a 10.98% increase in total cost. The impact a moderate amount of uncertainty has on the objective function value is similar between instances.

Table 4.3. OF values for the 10-node instances under maximum uncertainty

Uncertainty Values	Deterministic		RPRP-D		RPRP-TT		RPRP-DTT	
	0	0	10	0	0	12	10	12
Problem	OF		OF	%OF	OF	%OF	OF	%OF
10_1	171		174	1,66	217	26,87	218	27,73
10_2	205		207	0,81	253	23,23	254	23,98
10_3	200		202	0,60	242	20,95	243	21,55
10_4	190		192	0,75	232	22,19	234	22,90
10_5	176		177	0,67	219	24,54	220	25,21
10_6	215		216	0,75	265	23,33	266	24,02
10_7	190		198	4,28	235	23,47	242	27,14
10_8	223		225	0,88	266	19,54	268	20,42
10_9	175		176	0,58	218	24,90	219	25,48
10_10	190		192	0,75	234	22,88	235	23,62
Average	238		196	1,17	238	23,19	240	24,21
Std.Deviation	16,39		16,40		17,34		17,49	

The 10-node instances under maximum uncertainty show a stronger difference between the impact delays and increases in demand have on the total cost – on average, the increase of demand of all customers results in a slight increase of 1.17% in cost, while delays in travel time result in a 23.19% increase in total cost. The two uncertainties are mostly independent, as when both happen simultaneously the impact in the OF value is close to the sum of the two individual problems. However, the impact delays have on operation cost is

partially avoidable: all models were run with the assumption that the engine is left running when a vehicle is at a standstill, and, as previously discussed, the impact of keeping the engine running has on the objective function is shown in Figure 4.1.

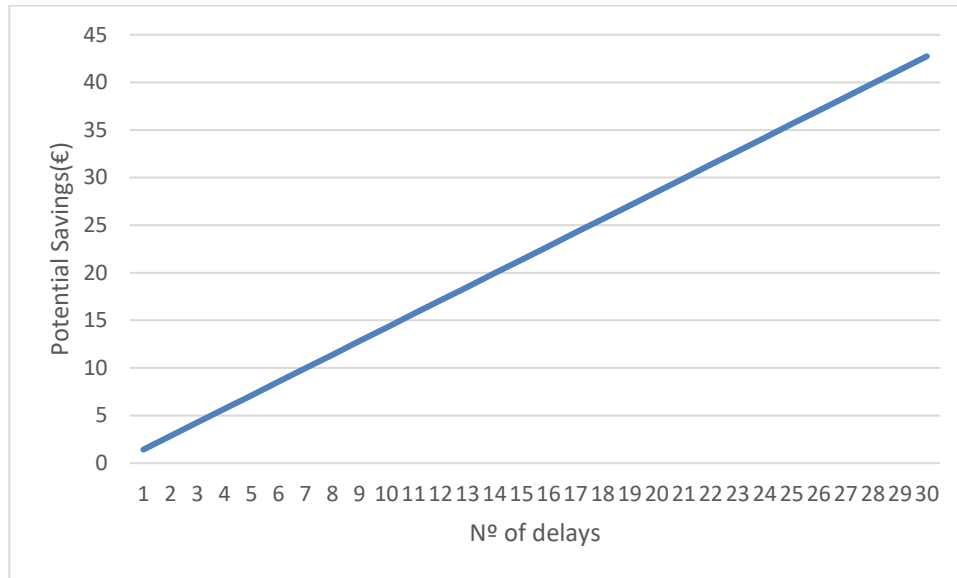


Figure 4.1. Reduction in operation costs resulting of shutting the engine down

When 6 arcs suffer a delay the impact of keeping the engine running in the OF is 8.55 euros, when 12 arcs suffer a delay, the impact is 17.09 euros. Such values are considerable and can easily be avoided by simply shutting the engine down when stopped. Table 4.4 shows the impact shutting the engine down has on the OF. In the following table “OF” represents the value obtained for the objective function, “OF-SS” is the value of the objective function for the same route when *start-stop* system is active, and “%OF-SS” is the percentual difference between “OF” and “OF-SS”.

Table 4.4. Savings caused by shutting the engine down in 10-node instances

Problem	RPRP-TT						RPRP-DTT					
	0			6			0			12		
	OF	OF-SS	%OF-SS	OF	OF-SS	%OF-SS	OF	OF-SS	%OF-SS	OF	OF-SS	%OF-SS
10_1	192	184	4,45%	217	200	7,89%	193	184	4,44%	218	201	7,83%
10_2	226	218	3,78%	253	236	6,76%	227	218	3,77%	254	237	6,72%
10_3	221	212	3,88%	242	225	7,06%	221	212	3,87%	243	226	7,02%
10_4	211	202	4,06%	232	215	7,36%	211	202	4,05%	234	217	7,32%
10_5	197	189	4,34%	219	202	7,81%	197	189	4,33%	220	203	7,77%
10_6	234	226	3,65%	265	248	6,46%	234	226	3,65%	266	249	6,43%
10_7	212	204	4,03%	235	218	7,28%	212	204	4,02%	242	225	7,07%
10_8	244	236	3,50%	266	249	6,43%	245	237	3,49%	268	251	6,38%
10_9	196	188	4,35%	218	201	7,84%	197	188	4,34%	219	202	7,80%
10_10	212	203	4,04%	234	217	7,32%	212	204	4,03%	235	218	7,27%
Average	215	206	4,01%	238	221	7,22%	215	206	4,00%	240	223	7,16%

When 6 delays are considered, shutting down the engine leads to a reduction in total operation costs averaging 4%, irrelevantly of whether demand uncertainty happens or

not. When uncertainty increases, so does the impact of stopping the engine – there is on average a 7% reduction in the total costs.

Such reductions are easy to achieve – modern vehicles possess a *start-stop* system, that automatically stops the car when it is at a standstill. These results show the relevance of this system to logistic companies, as they incur a smaller cost when faced with the inevitable delays on their delivery routes.

Table 4.5. Runtime values for 10-node instances under some uncertainty

Uncertainty Values	Deterministic		RPRP-D		RPRP-TT		RPRP-DTT	
	0	0	5	0	0	6	5	6
Problem	Time		Time	%Time	Time	%Time	Time	%Time
10_1	26		35	31,51	141	433,23	136	414,33
10_2	13		20	50,80	60	349,47	101	665,04
10_3	50		72	45,55	138	177,77	153	209,11
10_4	31		44	42,82	80	162,84	109	256,43
10_5	80		136	69,84	266	233,08	487	510,58
10_6	30		36	21,04	77	160,84	114	286,39
10_7	19		29	50,03	72	269,90	105	442,95
10_8	15		22	47,53	48	225,86	48	226,92
10_9	11		14	29,30	38	256,60	35	229,03
10_10	12		24	96,71	43	246,29	51	308,85
Average	29		43	48,51	96	251,59	134	354,96
Std.Deviation	20,42		34,52		66,03		123,36	

Table 4.6. Runtime values for 10-node instances under maximum uncertainty

Uncertainty Values	Deterministic		RPRP-D		RPRP-TT		RPRP-DTT	
	0	0	10	0	0	12	10	12
Problem	time		Time	%Time	Time	%Time	Time	%Time
10_1	26		33	25,33	170	544,32	192	628,30
10_2	13		18	32,58	84	531,95	115	766,86
10_3	50		45	-10,16	130	161,52	128	157,97
10_4	31		36	16,87	81	164,30	72	133,67
10_5	80		81	0,87	348	336,08	300	276,37
10_6	30		25	-16,11	158	432,83	162	447,23
10_7	19		34	75,03	71	264,61	98	404,02
10_8	15		17	14,91	55	270,05	66	344,72
10_9	11		10	-1,33	33	213,65	32	203,52
10_10	12		12	-5,22	41	232,86	42	237,07
Average	29		31	13,28	117	315,22	121	359,97
Std.Deviation	20,42		19,70		88,99		76,97	

The time increase in solving instances follows some of the patterns as the OF value increase, where demand uncertainty has a smaller impact in computational time, while travel time uncertainty in some instances takes almost five times as long to solve, when compared to deterministic version. However, when solving instances with demand and travel time uncertainty, the solving time suffers a larger increase than the sum of the previous two increases, being on average 359.97% slower than the original problem. The impact travel time uncertainty has on CPU runtimes varies greatly depending on the instance.

Table 4.7. OF values for 20-node instances under maximum uncertainty

Uncertainty Values	Deterministic		RPRP-D		RPRP-TT		RPRP-DTT	
	0	0	20	0	0	23	20	23
Problem	OF		OF	%OF	OF	%OF	OF	%OF
20_1	324		342	5,42	414	27,76	430	32,75
20_2	334		334	0,08	417	24,75	418	25,26
20_3	208		219	5,55	288	38,63	307	47,72
20_4	326		340	4,28	420	28,82	422	29,65
20_5	298		300	0,64	379	27,40	387	29,90
20_6	356		359	0,84	434	22,14	439	23,43
20_7	229		234	2,16	318	38,68	316	37,83
20_8	278		308	10,70	362	30,14	388	39,69
20_9	326		340	4,21	436	33,64	426	30,79
20_10	293		301	2,62	389	32,54	387	32,07
Average	297		308	3,65	386	30,45	392	32,91
Std.Deviation	45		45		47		44	

The impact both uncertainties have on the problems stays the same, when considering instances with more customers. On average, uncertainty in demand results in an increase of 3.65% in cost, while delays in travel time result in a 30.45% increase in total cost, with the impact of both uncertainties happening at the same time is close to the sum of the impacts of each type of uncertainty. However, the percentual increase in cost driven by demand uncertainty is quite variable, sometimes provoking a 10% worse value in OF, and sometimes having a negligible impact. On the contrary, the effect of delays is less dependent on the instance.

Table 4.8. Savings caused by shutting the engine down 20-node instances

Problem	RPRP-TT			RPRP-DTT		
	0		23	20		23
	OF	OF-SS	%OF-SS	OF	OF-SS	%OF-SS
20_1	414	381	7,92%	430	397	7,62%
20_2	417	384	7,86%	418	386	7,83%
20_3	288	255	11,37%	307	274	10,67%
20_4	420	387	7,81%	422	390	7,76%
20_5	379	346	8,64%	387	354	8,48%
20_6	434	402	7,54%	439	406	7,46%
20_7	318	285	10,31%	316	283	10,38%
20_8	362	329	9,06%	388	355	8,44%
20_9	436	403	7,52%	426	393	7,69%
20_10	389	356	8,43%	387	354	8,46%
Average	386	353	8,65%	392	359	8,48%

As shown in Table 4.8, the impact of engine stop in 20-node problems is slightly larger than the one in the worst case in the 10-node problem – there is on average more than

8% reduction in operation costs when start-stop systems are used. However, there is a larger variation of savings within 20-node instances. Table 4.9 shows the impact shutting the engine down has on the OF value, with “*Gap(%)*” indicating the percentual gap between the obtained solution and possible best solution.

Table 4.9. CPU runtime values for 20-node instances under maximum uncertainty

Uncertainty Values	Deterministic		RPRP-D		RPRP-TT		RPRP-DTT	
	0	0	20	0	0	23	20	23
Problem	Gap(%)		Gap(%)		Gap(%)		Gap(%)	
20_1	23		26		33		33	
20_2	22		20		28		27	
20_3	26		27		35		37	
20_4	25		26		33		32	
20_5	26		24		32		31	
20_6	32		24		34		29	
20_7	24		23		33		31	
20_8	23		23		31		29	
20_9	21		24		32		30	
20_10	28		29		36		33	
Average	25		25		33		31	
Std.Deviation	3		2		2		3	

Solving times balloon when considering 20-node instances, not obtaining optimal solutions within three hours. Gaps remain the same when only demand uncertainty exists and increase when uncertainty in travel time is introduced.

4.2.2. RPRP-TTD with Formulation II

While theoretically important, the second formulation of the travel time delay suffers heavily from poor performance, compared to the Formulation I. The performance in similar instances will be soon compared, but this formulation suffers from lack of performance in another manner: formulating the model itself is computationally expensive, due to the combinations of service times that must be individually analyzed to see if they belong in the model. As previously mentioned in Section 3.2.2.1, implementing (126) requires studying $(\phi + 1)^{|N_0|}$ constraints to see which are valid, and, since the proposed simplifications could not be implemented, for a 10-node instance with maximum travel time delay, this means parsing through 137 858 491 849 constraints to see whether or not they are valid. As such an amount could not be done in acceptable time (models were not being completely generated within 24 hours) the following results contain only results for 10 node instances with some uncertainty.

Table 4.10 and Table 4.11 show the solutions and CPU runtimes for the 10-node instances. The meaning of column values is the same as previously described.

Table 4.10. OF values for 10-node instances under some uncertainty

Uncertainty Values Problem	Deterministic		RPRP-D		RPRP-TT		RPRP-DTT	
	0	0	5	0	0	6	5	6
	OF		OF	%OF	OF	%OF	OF	%OF
10_1	170,90		171,51	0,36	203,89	19,30	204,45	19,63
10_2	205,18		205,72	0,26	238,98	16,48	239,45	16,70
10_3	200,32		200,72	0,20	230,61	15,12	231,01	15,32
10_4	190,09		190,58	0,26	220,39	15,94	220,87	16,19
10_5	175,72		176,11	0,23	206,01	17,24	206,41	17,47
10_6	214,55		214,90	0,16	252,21	17,55	252,64	17,76
10_7	190,32		190,74	0,22	220,62	15,92	221,03	16,14
10_8	222,59		223,33	0,33	252,88	13,61	253,62	13,94
10_9	174,66		175,00	0,19	204,96	17,35	205,29	17,54
10_10	190,11		190,62	0,27	220,40	15,94	220,92	16,21
Average	193,44		195,69	0,25	238,05	16,44	240,01	16,69
Std. Deviation	16,39		16,43		17,36		17,41	

As expected, when only demand uncertainty is present, the solutions are equal to the ones obtained with the Formulation I in Table 4.2. However, when, travel time delay occurs, the OF value worsens, compared with Formulation I. This is consistent with the different definitions of uncertainty present in each model. While this model presents solutions that withstand all possible combinations of up to 6 delays, the first model only has to guarantee that a solution is capable of withstanding 6 specific delays, therefore, it can choose where the delays occur to obtain a better OF value, which comes at a cost of the solution robustness.

Table 4.11. Runtime values for 10-node instances under some uncertainty

Uncertainty Values Problem	Deterministic		RPRP-D		RPRP-TT		RPRP-DTT	
	0	0	5	0	0	6	5	6
	Time		Time	%Time	Time	%Time	Time	%Time
10_1	52,76		109,21	106,98	345,27	554,38	532,40	909,03
10_2	37,95		49,45	30,29	174,32	359,33	241,07	535,21
10_3	87,77		141,12	60,79	358,89	308,91	603,36	587,44
10_4	48,29		57,68	19,44	186,11	285,40	217,94	351,32
10_5	114,34		156,35	36,74	415,14	263,08	715,63	525,89
10_6	55,67		95,34	71,26	376,63	576,54	438,66	687,96
10_7	33,01		44,98	36,29	145,51	340,86	224,39	579,85
10_8	33,02		36,78	11,40	135,28	309,75	158,29	379,42
10_9	14,86		18,09	21,78	70,05	371,51	88,97	498,85
10_10	15,95		30,78	92,90	76,30	378,22	116,78	631,97
Average	49,36		73,98	48,79	228,35	374,80	333,75	568,70
Std. Deviation	29,53		45,90		124,90		209,94	

When considering solving times, this model is clearly inferior to the first one. On average, this model requires double the time to solve an instance, when compared to Formulation I. This is due to two factors: the model is more complex - while the first model

can easily assign delays to certain arcs in a solution, and deal with travel time uncertainty (due to the permissive arrival and departure times customers have in these instances), Formulation II does not have the same ease of solving, as it still must consider all possible arrival times, with or without delays. Moreover, the lack of the two subtour breaking constraints (64)-(65) hurt solving times.

Overall, the model with recursive arrival times, although it is a relevant formulation for considering polyhedral uncertainty in the PRP, requires further development: the insertion of the maximum service time constraints must be optimized, to formulate the model for larger instances or for higher levels of uncertainty, and constraints that optimize solving times must be reintroduced.

4.3. Results of Bi-Objective RPRP-TTD

As the objective functions are conflicting, there is no feasible solution that optimizes both objective functions simultaneously. Therefore, we need to characterize (totally or partially) the nondominated solution set constituting the Pareto front, i.e., the feasible solutions for which one can only improve an objective function accepting to degrade, at least, another objective function value. As the proposed model is a MILP model, an approximation of the Pareto front was found using the ε -constraint method : the objective function (136) was set as an increasingly more difficult constrain – decreasing in steps of one, and the objective function (132)-(135) was chosen to be optimized.

4.3.1. Bi-Objective RPRP-TTD

Figure 4.2 shows Pareto fronts for the instances of the problem 10_2, under different levels of uncertainty.

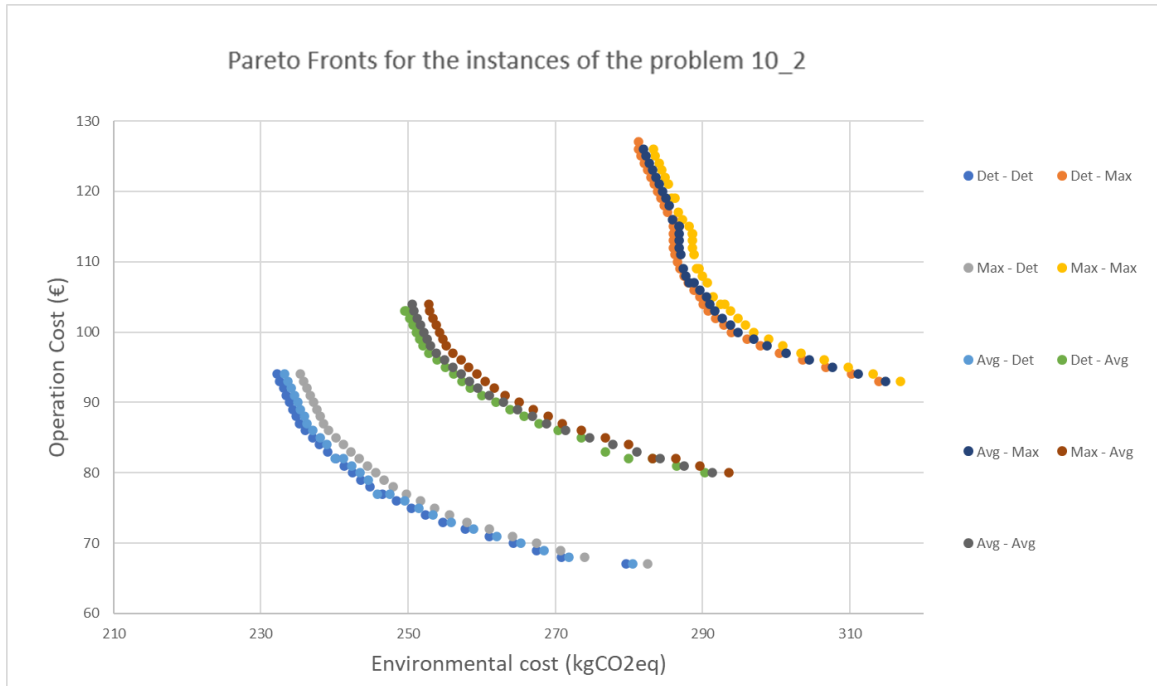


Figure 4.2. Pareto fronts for 10-node instances under different levels of uncertainty

Three groups of three Pareto fronts can be identified, where within each group all members have similar nondominated solution sets. The main distinction between members of different groups is the uncertainty in travel time: the leftmost group has certain travel times, the middle group has half of the arcs travelled suffering delays, and the rightmost group has the maximum number of arcs suffering delays. Within each group another pattern emerges: an increase in demand uncertainty drives a slight worsening of the Pareto front (when compared to an increase in travel time uncertainty). This means that increasing delays in routes have a more adverse effect in the total operation cost. A similar saving through the *start-stop* mechanism can be applied to the emissions of each solution. The savings have increasing impact in the third group, but they have no other effect than bringing the groups closer.

Figure 4.3 shows Pareto fronts for the different instances of the problem 20_1, under different levels of uncertainty.

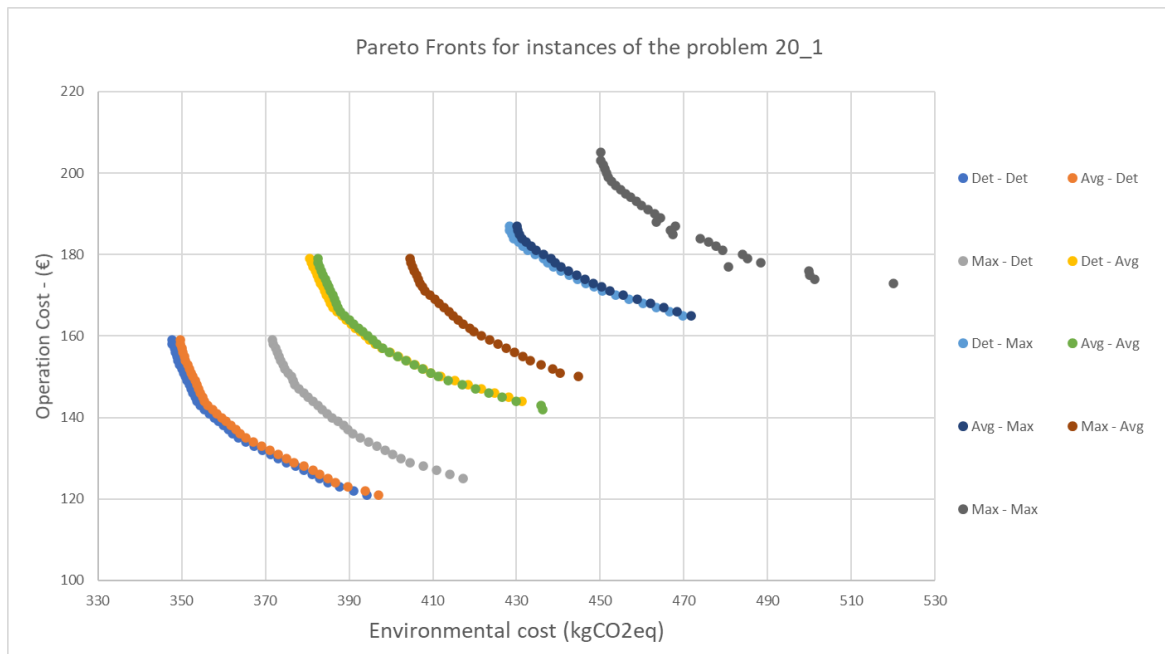


Figure 4.3. Pareto fronts for 20-node instances under different levels of uncertainty

When increasing the number of customers, the same three groups distinguished by the level of travel time uncertainty remain; however, the impact of demand uncertainty changes drastically: while some uncertainty leads to marginally worse solution space, maximum uncertainty severely worsens the operation environmental performance, having no effect in operation costs, in the cases where only some arcs have uncertain travel times. When the worst-case scenario is reached in both cases – not only is the environmental performance worse, but the increase in requirements coupled with the many delays necessitate the inclusion of another vehicle.

4.3.2. Impact of increasing delay amount

Although previous results were obtained using 1000 seconds delay, in the real-world delays may be distinct, and the impact of different delays can be different, and not reduced only to somewhat increasing emissions and driver cost. Multiple instances of one 10-node and one 20-node problem were run, where the maximum time travel delay was considered, but each time the delay magnitude increased. Instances were initially run with 500 seconds delay and an increase of 100 seconds was applied, until 2000 seconds were reached.

Figure 4.4 shows Pareto fronts for the instances of the problem 10_2, with maximum uncertainty and increasing delay amounts.

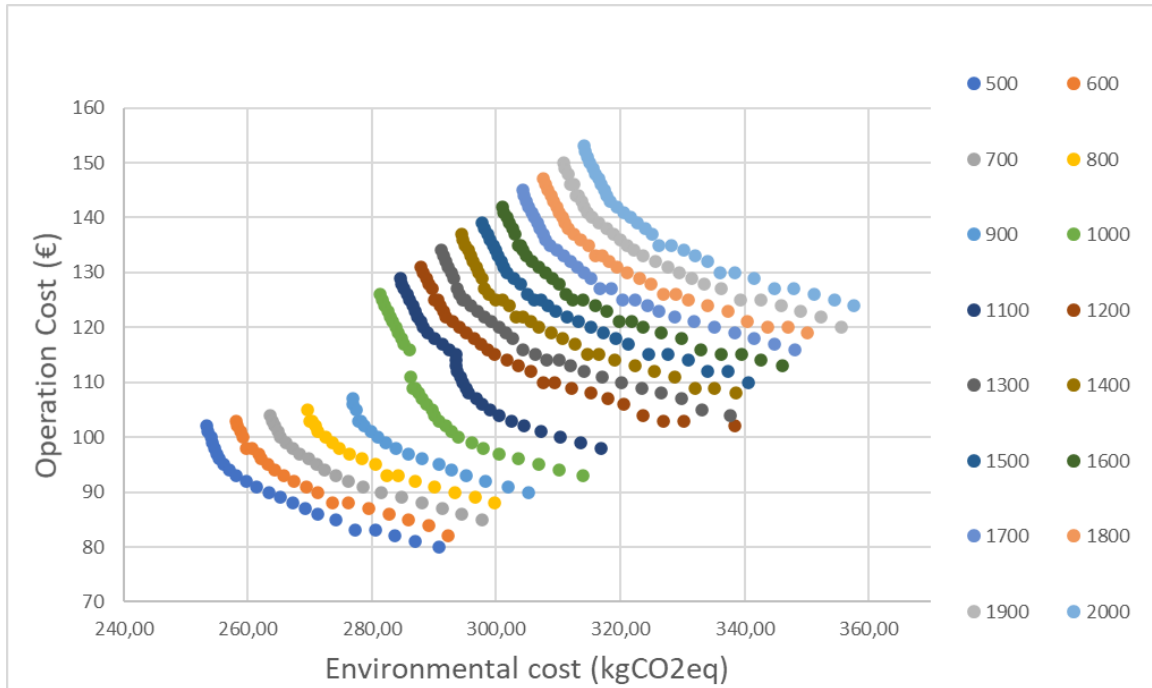


Figure 4.4. Pareto fronts for a 10-node instance under maximum uncertainty with increasing delay amount

When studying the effect of the delay amount has in this instance, we can easily distinguish two groups: one composed of delays under 1000 seconds, and another with delays equal or greater than 1000 seconds. The former has Pareto fronts of similar shape, with each one being a slightly worse version of the previous. This is due to the impact a delay has on fuel consumption and travel time, while the routes obtained remain mostly the same within this group. Increasing the delay magnitude results in more time the engine is running while the car is at a standstill, and in an increase in service time. However, when jumping from 900 seconds delay to 1000 seconds, there is a drastic change in the nondominated solutions – while the minimum amount possible of operation costs remains a linear increase from the previous minimum, minimizing emissions now results in a sharp increase in driver costs. This is because minimization of fuel consumption, which is correlated with emissions minimization, happens at a speed below the maximum amount, and with delays larger than 900 seconds three vehicles no longer can satisfy the time constraints of all customers, requiring another vehicle, that leads to a strong increase in the driver cost. Delay amounts larger than 1200 seconds contain only solutions with 4 vehicles and delays smaller than 1000 seconds contain only solutions with 3 vehicles. Delays of 1100

and 1200 seconds are particularly important, as they show the differences between routes of 3 and 4 vehicles, which are shown in Figure 4.5, alongside with 900 and 1300 second delays for comparison.

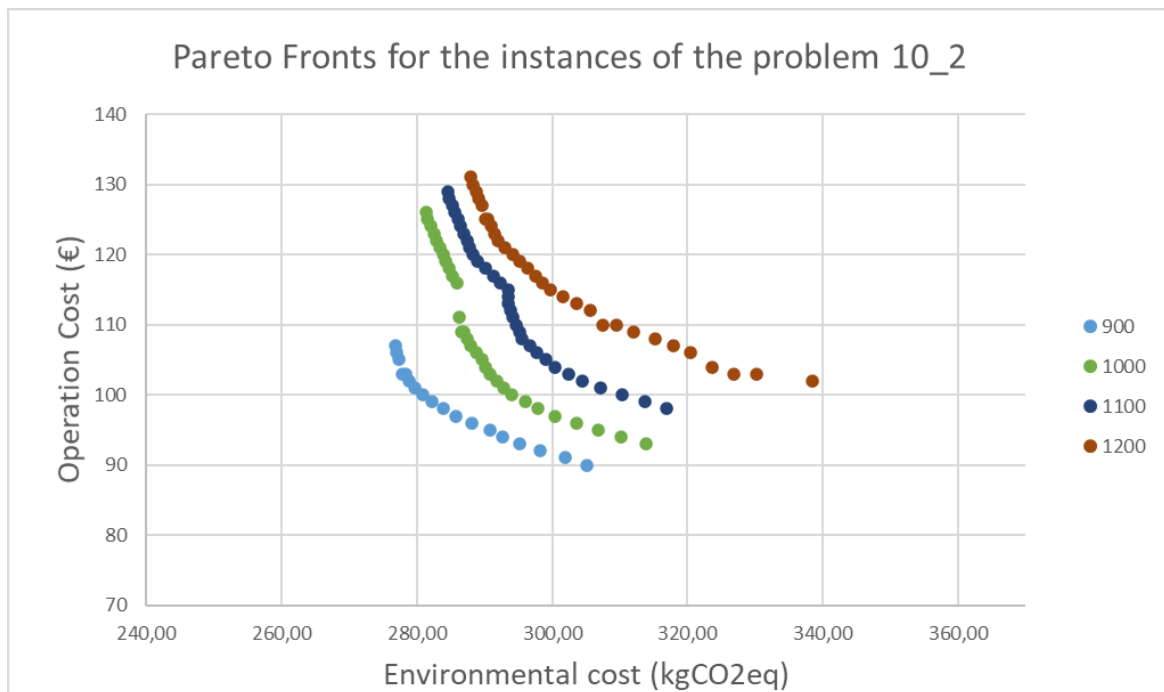


Figure 4.5. Pareto fronts for a 10-node instance under maximum uncertainty with increasing delay amount

Delays of 1000 and 1100 seconds are the only ones that contain solutions with 3 and 4 vehicles, and the change between the two values can be seen in their Pareto fronts: when the main aim is to minimize emissions, both run 4 cars, and are shaped similarly to solution spaces with 1200 seconds delay or larger, which allows them to attain optimal speed, and reduce emissions. However, at a certain point (operation cost below 116€) such operation costs cannot be attained with four drivers, and solutions change to using three vehicles only, with the rest of the Pareto front taking similar shape as the ones created with delays 900 seconds or lower.

Figure 4.6 shows the Pareto fronts for the instances of the problem 20_1, with maximum uncertainty and increasing delay amounts.

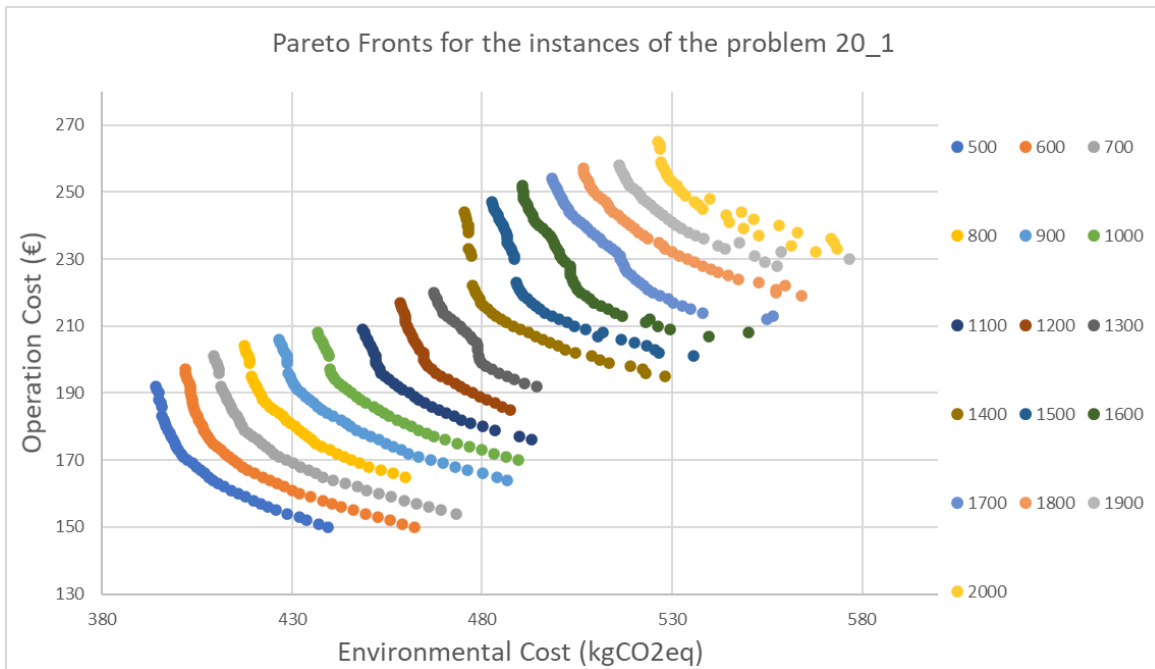


Figure 4.6. Pareto fronts for a 20-node instance under maximum uncertainty with increasing delay amount

Similarly to the 10-node problem, we can distinguish two groups: one composed of delays under 1300 seconds, and another one with delays equal or greater than 1400 seconds. The former has Pareto fronts of similar shape, with each one being a slightly worse version of the previous one. However, when jumping from 1300 seconds delay to 1400 seconds, there is a drastic change in the nondominated solutions – while the minimum amount possible of operation costs remains a small increase from the previous minimum, minimizing emissions results in a sharp increase in driver costs, due to an increase in the number of vehicles.

5. CONCLUSION

In this dissertation we developed a collection of models for the Pollution Routing Problem with travel time and demand uncertainty, defining the impact each type of uncertainty has on the objective function, thus extending robustness approaches to green routing problems.

5.1. Main contributions

By using several robust techniques, we have showed that it is possible to deal with data uncertainty and to obtain reliable solutions with a limited worsening of the objective function values. Obtaining solutions that are robust for demand uncertainty only marginally increases operation costs. Solutions unaffected by travel time uncertainty have a greater effect on operation cost. Therefore, the DM should carefully evaluate between robustness vs. optimality of solution.

We also showed that the benefits of stopping the engine when at a standstill: reduce total operation cost by 4% when some delays happen, and the impact increases with the number of delays.

Using the shown robust techniques, companies can reduce the risk of unmet demand and late arrivals. While solutions obtained with this method are more costly when compared with non-robust solutions, when realized, non-robust solutions may fail, and result in unsatisfied customers and extra operation costs. The solution robustness can also be controlled, allowing for the DM to find a balanced point in between solution robustness and optimal routing.

We also showed obtaining robust solutions has a different impact on objective functions tradeoff – while demand uncertainty results only in a worsening of emissions, travel time uncertainty worsens both environmental and travel time performance. However, while obtaining reliable solutions for different uncertainties has different impacts on the Pareto front, its shape remains similar for different uncertainty levels. The impact of an increase in delay is also studied, and remains stable until a certain threshold is reached, at

which an increase in the number of vehicles is necessary, which results in a stronger worsening of the Pareto front, and a change in its shape.

5.2. Future Work

The most extensively researched model in this dissertation, Formulation I, while simple to implement, suffers from demand and travel time variables not belonging to a polyhedral uncertainty set, which reduces the robustness of solutions with some uncertainty obtained with this formulation. While this has been partially addressed with Formulation II, the second model is difficult to formulate and to solve, and only guarantees polyhedral uncertainty for travel time delays. Expanding this model to include demand uncertainty and optimizing its creation and solving times are both two possible avenues of research.

REFERENCES

- Bektaş, T., & Laporte, G. (2011). The Pollution-Routing Problem. *Transportation Research Part B: Methodological*, 45(8), 1232–1250.
<https://doi.org/10.1016/j.trb.2011.02.004>
- Ben-Tal, A., & Nemirovski, A. (2000). Digital Object Identifier (DOI) 10.1007/s101070000163. *Math. Program., Ser. A*, 88, 411–424.
<https://doi.org/10.1007/s101070000163>
- Bertsimas, D., & Sim, M. (2004). The price of robustness. *Operations Research*, 52(1), 35–53. <https://doi.org/10.1287/opre.1030.0065>
- Charnes, A., Cooper, W. V., & Cooper3, W. W. (1959). CHANCE-CONSTRAINED PROGRAMMING A. CHARNES2 a n d. In *Management Science* (Vol. 6, Issue 1).
- Cordeau, J.-F., Desautniers, G., Desrosiers, J., Solomon, M. M., & Soumis, F. (1999). *The VRP with Time Windows*.
- Dantzig, G. B., & Ramser, J. H. (1959). The Truck Dispatching Problem. In *Source: Management Science* (Vol. 6, Issue 1).
- Demir, E., Bektaş, T., & Laporte, G. (2012). An adaptive large neighborhood search heuristic for the Pollution-Routing Problem. *European Journal of Operational Research*, 223(2). <https://doi.org/10.1016/j.ejor.2012.06.044>
- Demir, E., Bektaş, T., & Laporte, G. (2014). The bi-objective Pollution-Routing Problem. *European Journal of Operational Research*, 232(3).
<https://doi.org/10.1016/j.ejor.2013.08.002>
- Erdoğan, S., & Miller-Hooks, E. (2012). A Green Vehicle Routing Problem. *Transportation Research Part E: Logistics and Transportation Review*, 48(1), 100–114. <https://doi.org/10.1016/j.tre.2011.08.001>
- Eshtehadi, R., Fathian, M., & Demir, E. (2017). Robust solutions to the pollution-routing problem with demand and travel time uncertainty. *Transportation Research Part D: Transport and Environment*, 51. <https://doi.org/10.1016/j.trd.2017.01.003>
- Franceschetti, A., Honhon, D., van Woensel, T., Bektaş, T., & Laporte, G. (2013). The time-dependent pollution-routing problem. *Transportation Research Part B: Methodological*, 56. <https://doi.org/10.1016/j.trb.2013.08.008>
- Koç, Ç., Bektaş, T., Jabali, O., & Laporte, G. (2014). The fleet size and mix pollution-routing problem. *Transportation Research Part B: Methodological*, 70.
<https://doi.org/10.1016/j.trb.2014.09.008>
- Laporte, G. (1992). The vehicle routing problem: An overview of exact and approximate algorithms. *European Journal of Operational Research*, 59(3).
[https://doi.org/10.1016/0377-2217\(92\)90192-C](https://doi.org/10.1016/0377-2217(92)90192-C)
- Li, X., Tian, P., & Leung, S. C. H. (2010). Vehicle routing problems with time windows and stochastic travel and service times: Models and algorithm. *International Journal of Production Economics*, 125(1). <https://doi.org/10.1016/j.ijpe.2010.01.013>
- Li, Z., Floudas, C. A. (2012). Robust Counterpart Optimization: Uncertainty Sets, Formulations and Probabilistic Guarantees. *Proceedings of 6th Conference on Foundations of Computer-Aided Process Operations*.

- Moryadee, C., Aunyawong, W., & Shaharudin, M. R. (2019). Congestion and Pollution, Vehicle Routing Problem of a Logistics Provider in Thailand. *The Open Transportation Journal*, 13(1). <https://doi.org/10.2174/1874447801913010203>
- Munari, P., Moreno, A., de La Vega, J., Alem, D., Gondzio, J., & Morabito, R. (2019). The robust vehicle routing problem with time windows: Compact formulation and branch-price-and-cut method. *Transportation Science*, 53(4). <https://doi.org/10.1287/trsc.2018.0886>
- Nasri, M., Hafidi, I., & Metrane, A. (2020). Multithreading parallel robust approach for the vrptw with uncertain service and travel times. *Symmetry*, 13(1), 1–16. <https://doi.org/10.3390/sym13010036>
- Nasri, M., Metrane, A., Hafidi, I., & Jamali, A. (2020). A robust approach for solving a vehicle routing problem with time windows with uncertain service and travel times. *International Journal of Industrial Engineering Computations*, 11(1), 1–16. <https://doi.org/10.5267/j.ijiec.2019.7.002>
- Nath, R., Rauniyar, A., Muhuri, P. K., & Shukla, A. K. (2019). A Novel Bilevel Formulation for Pollution Routing Problem. *Proceedings of the 2018 IEEE Symposium Series on Computational Intelligence, SSCI 2018*. <https://doi.org/10.1109/SSCI.2018.8628725>
- Oyola, J., Arntzen, H., & Woodruff, D. L. (2018). The stochastic vehicle routing problem, a literature review, part I: models. *EURO Journal on Transportation and Logistics*, 7(3). <https://doi.org/10.1007/s13676-016-0100-5>
- Peng, B., Wu, L., Yi, Y., & Chen, X. (2020). Solving the multi-depot green vehicle routing problem by a hybrid evolutionary algorithm. *Sustainability (Switzerland)*, 12(5). <https://doi.org/10.3390/su12052127>
- Poonthalir, G., & Nadarajan, R. (2018). A Fuel Efficient Green Vehicle Routing Problem with varying speed constraint (F-GVRP). *Expert Systems with Applications*, 100. <https://doi.org/10.1016/j.eswa.2018.01.052>
- Qiu, R., Xu, J., Ke, R., Zeng, Z., & Wang, Y. (2020). Carbon pricing initiatives-based bi-level pollution routing problem. *European Journal of Operational Research*, 286(1). <https://doi.org/10.1016/j.ejor.2020.03.012>
- Rouky, N., Boukachour, J., Boudebous, D., & Alaoui, A. E. H. (2018). A Robust Metaheuristic for the Rail Shuttle Routing Problem with Uncertainty: A Real Case Study in the Le Havre Port. *Asian Journal of Shipping and Logistics*, 34(2), 171–187. <https://doi.org/10.1016/j.ajsl.2018.06.014>
- Soyster, A. L. (1973). Technical Note—Convex Programming with Set-Inclusive Constraints and Applications to Inexact Linear Programming. *Operations Research*, 21(5), 1154–1157. <https://doi.org/10.1287/opre.21.5.1154>
- Tajik, N., Tavakkoli-Moghaddam, R., Vahdani, B., & Meysam Mousavi, S. (2014). A robust optimization approach for pollution routing problem with pickup and delivery under uncertainty. *Journal of Manufacturing Systems*, 33(2). <https://doi.org/10.1016/j.jmsy.2013.12.009>
- Wang, A., Subramanyam, A., & Gounaris, C. E. (2021). Robust vehicle routing under uncertainty via branch-price-and-cut. *Optimization and Engineering*. <https://doi.org/10.1007/s11081-021-09680-6>
- Xiao, Y., Zuo, X., Huang, J., Konak, A., & Xu, Y. (2020). The continuous pollution routing problem. *Applied Mathematics and Computation*, 387. <https://doi.org/10.1016/j.amc.2020.125072>

- Yu, Z., Zhang, P., Yu, Y., Sun, W., & Huang, M. (2020). An Adaptive Large Neighborhood Search for the Larger-Scale Instances of Green Vehicle Routing Problem with Time Windows. *Complexity*, 2020. <https://doi.org/10.1155/2020/8210630>
- Zhen, L., Xu, Z., Ma, C., & Xiao, L. (2020). Hybrid electric vehicle routing problem with mode selection. *International Journal of Production Research*, 58(2). <https://doi.org/10.1080/00207543.2019.1598593>